

2-6-96

SANDIA REPORT

SAND95-2871 • UC-704

Unlimited Release

Printed January 1996

RECEIVED

FEB 14 1996

OSTI

Epoxy and Acrylate Stereolithography Resins: In-Situ Property Measurements

T. R. Guess, R. S. Chambers, T. D. Hinnerichs

Prepared by
Sandia National Laboratories
Albuquerque, New Mexico 87185 and Livermore, California 94550
for the United States Department of Energy
under Contract DE-AC04-94AL85000

Approved for public release; distribution is unlimited.

Issued by Sandia National Laboratories, operated for the United States Department of Energy by Sandia Corporation.

NOTICE: This report was prepared as an account of work sponsored by an agency of the United States Government. Neither the United States Government nor any agency thereof, nor any of their employees, nor any of their contractors, subcontractors, or their employees, makes any warranty, express or implied, or assumes any legal liability or responsibility for the accuracy, completeness, or usefulness of any information, apparatus, product, or process disclosed, or represents that its use would not infringe privately owned rights. Reference herein to any specific commercial product, process, or service by trade name, trademark, manufacturer, or otherwise, does not necessarily constitute or imply its endorsement, recommendation, or favoring by the United States Government, any agency thereof or any of their contractors or subcontractors. The views and opinions expressed herein do not necessarily state or reflect those of the United States Government, any agency thereof or any of their contractors.

Printed in the United States of America. This report has been reproduced directly from the best available copy.

Available to DOE and DOE contractors from
Office of Scientific and Technical Information
PO Box 62
Oak Ridge, TN 37831

Prices available from (615) 576-8401, FTS 626-8401

Available to the public from
National Technical Information Service
US Department of Commerce
5285 Port Royal Rd
Springfield, VA 22161

NTIS price codes
Printed copy: A03
Microfiche copy: A01

DISCLAIMER

This report was prepared as an account of work sponsored by an agency of the United States Government. Neither the United States Government nor any agency thereof, nor any of their employees, makes any warranty, express or implied, or assumes any legal liability or responsibility for the accuracy, completeness, or usefulness of any information, apparatus, product, or process disclosed, or represents that its use would not infringe privately owned rights. Reference herein to any specific commercial product, process, or service by trade name, trademark, manufacturer, or otherwise does not necessarily constitute or imply its endorsement, recommendation, or favoring by the United States Government or any agency thereof. The views and opinions of authors expressed herein do not necessarily state or reflect those of the United States Government or any agency thereof.

SAND95-2871
Unlimited Release
Printed January 1996

Distribution
Category UC-704

EPOXY AND ACRYLATE STEREOLITHOGRAPHY RESINS: IN-SITU PROPERTY MEASUREMENTS

T. R. Guess
Organic Materials Department 1472

R. S. Chambers
Engineering and Manufacturing Mechanics Department 9117

T. D. Hinnerichs
Structural Dynamics Department 9234

Sandia National Laboratories
Albuquerque, NM 87185

ABSTRACT

Stereolithography is a rapid prototyping method that is becoming an important product realization and concurrent engineering tool, with applications in advanced and agile manufacturing. During the build process, material behavior plays a significant role in the mechanics leading to internal stresses and, potentially, to distortion (curling) of parts. The goal of the "*Stereolithography Manufacturing Process Modeling and Optimization*" LDRD program was to develop engineering tools for improving overall part accuracy during the stereolithography build process. These tools include phenomenological material models of solidifying stereolithography photocurable resins and a 3D finite element architecture that incorporates time varying material behavior, laser path dependence, and structural linkage. This SAND report discusses the in situ measurement of shrinkage and force relaxation behavior of two photocurable resins, and the measurement of curl in simple cantilever beams. These studies directly supported the development of phenomenological material models for solidifying resins and provided experimental curl data to compare to model predictions.

MASTER

DISTRIBUTION OF THIS DOCUMENT IS UNLIMITED 

TABLE OF CONTENTS

ABSTRACT	3
TABLE OF CONTENTS.....	5
LIST OF TABLES	6
LIST OF FIGURES	7
INTRODUCTION	10
MATERIALS AND STEREOLITHOGRAPHY EQUIPMENT	11
TEST METHODS AND RESULTS	11
AREA MEASUREMENTS	11
LINEAR SHRINKAGE MEASUREMENTS	12
Sandia Data	12
University of Dayton Data.....	13
FORCE MEASUREMENTS	13
SL 5149 Acrylate Data	14
SL 5170 Epoxy Data	15
BULK MATERIAL MEASUREMENTS	15
CURL MEASUREMENTS	16
SUMMARY	17
REFERENCES	18
ACKNOWLEDGMENTS	18
FIGURES	19
APPENDICES	33
APPENDIX A. University of Dayton Cure Shrinkage Data	33
APPENDIX B. SL 5170 Epoxy: Tests of Single Strands and Bulk Material	40
DISTRIBUTION	43

LIST OF TABLES

Table A1. Test Conditions for SL 5170 Trials- Data Set #1	35
Table A2. Summary of SL 5170 Linear Shrinkage Measurements- Data Set #1	35
Table A3. Cure Depth Measurements of SL 5149 Acrylate Resin	36
Table A4. Test Conditions for SL 5149 Trials.....	37
Table A5. Summary of SL 5149 Linear Shrinkage Measurements	37
Table B1. Initial Modulus of SL 5149 Acrylate Strands as a Function of Strain Rate and Post Cure Time	41
Table B2. Tensile Properties of SL 5170 Epoxy Strands as a Function of Strain Rate	42
Table B3. Elastic Properties of SL 5170 Epoxy Calculated Using Ultrasonic Wave Speeds	42

LIST OF FIGURES

Fig. 1. Schematic of stereolithography process.....	19
Fig. 2. 3D System's SLA-250 stereolithography apparatus with the door open showing location of force measuring fixture. Post curing chambers are on the right.....	19
Fig. 3. Expanded view of the force measuring fixture.....	20
Fig. 4. Typical cross sections of strands drawn with a single pass of a HeCd laser: (a) dark field image and b) binary image of SL 5170 epoxy; and (c) dark field image and d) binary image of SL 5149 acrylate. A scale marker of 0.003 inch length is shown in each image.....	20
Fig. 5. Cross sections of SL 5149 acrylate and SL 5170 epoxy strands for different number of laser hits. Arrow indicates direction of laser hit. Strands were not recoated between hits. A, W and D denote strand area, width (at widest point) and depth, respectively. A scale marker of 0.004 inch length is shown for each acrylate image and a 0.005 inch marker for each epoxy image.	21
Fig. 6. Strand cross sectional area as a function of number of laser hits.	21
Fig. 7. Schematic of setup for video measurement of strand linear shrinkage.	22
Fig. 8. View of strand tip using Schlieren method.....	22
Fig. 9. View of strand and tag using the glitter float method.....	23
Fig. 10. Linear shrinkage of SL 5170 epoxy: comparison of results from three different lengths of strands drawn in an SLA-250 stereolithography machine.....	23
Fig. 11. Linear shrinkage of SL 5149 acrylate: comparison of results from three different lengths of strands drawn in an SLA-250 stereolithography machine.....	24
Fig. 12. Schematic of experimental setup for force measurements and stress relaxation experiments.	24
Fig. 13. Forces developed in SL 5149 acrylate due to multiple hits of the laser and a 0.5% step strain to a 1.0 inch strand. Force relaxation occurs following the step strain.	25
Fig. 14. Cure shrinkage forces in a 1.0 inch SL 5149 acrylate strand due to multiple hits of the laser.	25
Fig. 15. Expanded view of cure shrinkage forces in the Figure 14 acrylate strand.....	26
Fig. 16. Initial modulus of SL 5149 acrylate as function of number of laser hits.....	26

Fig. 17. Initial modulus of SL 5149 acrylate and SL 5170 epoxy as a function of time following a single laser hit of a strand. The strand remains in the resin vat during the time interval between the draw and the tensile test.....	27
Fig. 18. Stress relaxation measured in single strands of SL 5149 acrylate resin following multiple laser hits (stress in psi and time in seconds)..	27
Fig. 19. Stress vs. strain response of SL 5170 epoxy strands for different number of laser hits.	28
Fig. 20. Initial modulus of SL 5170 epoxy strands as a function of elapsed time from the 1st laser hit.....	28
Fig. 21. Force relaxation of SL 5170 epoxy. Step strain of 0.5% applied to strand at different times following the laser draw of a strand. The strand remains in the resin vat during the time interval between the draw and the tensile force relaxation test.	29
Fig. 22. Force relaxation of SL 5170 epoxy. Step strain of 0.5% applied to strand at different times following the laser draw of a strand. The strand remains in the resin vat during the time interval between the draw and the tensile force relaxation test.	29
Fig. 23. Dimensions (inches) of SL 5149 acrylate cantilever beam specimen for distortion (curl) measurements.	30
Fig. 24. Schematics illustrating the vector paths and drawing sequence for the two build styles curl measurement specimens. Analysis of the cantilever beams and comparison between experiment and calculations are discussed in Reference [3].	30
Fig. 25. Representative picture of SL 5149 acrylate cantilever beams from the two build styles, the beams were not post cured.: (a) Build Style I cantilever beam, (b) Build Style II cantilever beam	31
Fig. 26. Measured out-of-plane curl of SL 5149 acrylate Build Style I and Build Style II cantilever beams	32

FIGURES IN APPENDICES

Fig. A1. Schematic of the University of Dayton apparatus for measuring real time shrinkage during curing.....	37
Fig. A2. SL 5170 epoxy resin shrinkage vs. log time; the data are averages of the four trials. The first 30 ms exposure occurs at time zero and the second 30 ms exposure occurs at 300 s.....	38

Fig. A3. SL 5149 acrylate resin shrinkage vs. log time for trial having a 5 minute wait between 10 ms exposures. (Vat temperature = 30°C, relative humidity = 40% measured at 23°C, and laser power at the vat = 16 mW.)	38
Fig. A4. SL 5149 acrylate resin shrinkage vs. log time for trial having a 10 minute wait between exposures. Data was collected for 10 minutes after second exposure. Vat temperature = 30°C, relative humidity = 34% measured at 22°C, and laser power at the vat = 16 mW.)	39
Fig. A5. SL 5149 acrylate resin shrinkage vs. log time for trial having a 1 second wait between the two 10 ms exposures.	39
Fig. B1. Tensile stress-strain responses of SL 5149 acrylate single strands tested in an Instron machine at three strain rates. A 250 gram load cell and a 3.0 inch gage length used in the tests. Strands removed from SLA-250 vat 5 minutes after laser draw and post cured for 1 hour in a UV chamber prior to tests.	40
Fig. B2. Typical tensile stress-strain responses of SL 5149 acrylate dogbone specimens as a function of strain rate	41

INTRODUCTION

Stereolithography is a rapid prototyping process in which three dimensional (3D) parts are built by selectively curing successive layers of liquid photosensitive resin, one on top of another [1]. The geometric definition of the layers is obtained by constructing a series of slices through a 3D solid computational model of a part. These slices, when reconstructed in sequence, reproduce the full part geometry. Working from a slice definition file, the stereolithography apparatus (SLA) uses a focused ultraviolet (UV) laser beam directed by a computer-controlled X-Y scanning mirror system to accurately trace the layer geometry on the surface of the resin. As the laser spot passes over the surface of the resin, the ensuing chemical reaction causes the resin to shrink and stiffen during solidification. A schematic diagram of the process can be seen in Figure 1. As with any rapid-prototyping method where solidifying materials undergo shrinkage, dimensional accuracy can be difficult to maintain. When laser paths within a layer cross or when new layers are cured on top of existing layers, residual stresses are generated as the cure shrinkage of the freshly gelled resin is resisted by the stiffness of the adjoining previously-cured material. These internal stresses, though small, can cause significant deformations (curling) in the compliant material. The presence of such deformations can lead to distorted parts that do not comply with specified geometric accuracy requirements.

An LDRD program entitled "*Stereolithography Manufacturing Process Modeling and Optimization*" proposed to develop and evaluate the use of engineering tools for modeling curl and studying parameters that might improve overall build accuracy in stereolithography parts. These tools include phenomenological material models of the solidifying resins and a 3D finite element model that incorporates time varying material behavior, laser path dependence, and structural linkage. Results of 1) the development of a 3D finite element code architecture to numerically simulate part-building in the stereolithography process, and 2) the investigation of the possibility of analyzing part-building using a simple phenomenological model of solidifying resins are reported elsewhere [2, 3].

This report describes the experimental portion of the LDRD program; both single strand and bulk material properties are reported. Methods developed to measure the in situ response of polymer strands laser drawn in a commercial SLA have been reported [4, 5]. These methods are discussed and data for two different photocurable resins are presented in this report. The data include cross-sectional areas, linear shrinkage, initial modulus and stress relaxation response of individual strands of epoxy and acrylate stereolithography resins. In addition, out-of-plane curl of acrylate cantilever beam specimens, built with two different draw styles are discussed.

MATERIALS AND STEREOLITHOGRAPHY EQUIPMENT

Two Ciba Geigy resins, Cibatool® SL 5170 and Cibatool® SL 5149, were used in the experimental study. SL 5170 is an epoxy and SL 5149 is an acrylate ester. Both materials are one-component, photo curable liquid resins designed for helium cadmium (HeCd) laser-based stereolithography equipment, especially for 3D Systems' SLA-250.

Strand specimens were drawn in a 3D System's SLA-250 stereolithography machine, Figure 2. To facilitate the in situ experiments on single strands, the large resin vat of a conventional SLA-250 system was removed and a platform was inserted in its place. This platform was used to support smaller reservoirs of resin and specialized test fixtures for linear shrinkage and force measurement tests, Figure 3. Strand specimens are drawn with a single pass of the laser beam. At times, this step was repeated to produce multiple laser exposures or hits on a single strand. During multiple exposure experiments, the strand was not recoated with fresh resin between laser hits.

The SLA-250 utilizes a HeCd laser that builds with a draw velocity that is dependent on laser power and a specified depth of cure; draw velocity was about 1 in/s for a 16 mW laser and 0.008 inch cure depth in epoxy resin. During linear shrinkage experiments at the beginning of the study, nominal laser power was 16 mW. Prior to force response experiments, the 16 mW laser malfunctioned and was replaced with one having nominal 30 mW of power; draw velocity in this system approached 20 in/s. Drawing parameter inputs to the SLA-250 were set at 0.008 inch cure depth for SL 5170 epoxy and at 0.010 inch for SL 5149 acrylate.

TEST METHODS AND RESULTS

Property measurements were made in situ within the SLA-250 on single strands and outside the SLA-250 on bulk samples built by the stereolithography process. Methods are presented for in situ measurement of linear shrinkage, initial modulus and stress relaxation of single strands. Because load bearing areas are required for stress calculations, a procedure to measure strand cross sectional areas is also described.

AREA MEASUREMENTS

Metallography techniques were developed to determine the shapes and areas of SL 5170 epoxy and SL 5149 acrylate strands drawn in the SLA-250. A drawn strand is removed from the resin and excess resin is gently wiped from it with an alcohol soaked Q-tip. The flexible strand specimen is placed in an epoxy-wetted groove on a rigid glass epoxy substrate for support. The substrate is then potted inside a one inch diameter mold ring using Epon 815/3404 epoxy; the epoxy potting is cured at room temperature for 6 hours.

The potted specimen is prepared for metallographic inspection by a series of four grinding and polishing steps between bonded diamond platens using abrasive sizes of 30 μm , 15 μm , 6 μm , and 1 μm , respectively. A final polish with 0.6 μm colloidal silica suspension on a nylon

cloth removes any smearing that may have occurred in the softer strand. Dark field images yield the clearest definition of the strand boundary. A binary image is taken from the metallographic image and used for dimension and area measurements.

These techniques are used to measure epoxy and acrylate strands made with single and multiple passes of the laser. Typical metallographic and binary images of epoxy and binary images of acrylate strands following a single laser hit are shown in Figure 4; examples of binary images following multiple hits of the laser are shown in Figure 5. Curves of strand area as a function of number of laser hits are plotted in Figure 6. Note that the cross sectional area of the epoxy increases at a higher rate than the acrylate area does.

LINEAR SHRINKAGE MEASUREMENTS

Sandia Data

Time history linear shrinkage of SL 5170 epoxy and SL 5149 acrylate strands are obtained by measuring the change in length of individual strands after gelation. Measurements are made in situ on strands of up to 1.5 inches length that are polymerized by a single pass of the laser spot. A non-contact video method was developed to make the shrinkage measurements. It was observed that a drawn strand affects the flatness of the resin pool surface and that a slight index difference exists between the cured strand and the uncured resin bath. These properties permit a Schlieren-like technique for viewing the shrinking strand following the laser draw.

Figure 7 illustrates the experimental arrangement. A small reservoir of resin is imaged at 1 to 1 magnification using a miniature video camera. Light from a fiber optic bundle illuminates the resin surface with the incident angle chosen to reflect light into the lens aperture. A VHS video cassette recorder captures the video images at 30 images per second.

As the material begins to polymerize after the laser draw, the surface flatness of the uncured resin is disturbed. Therefore, light rays reflected from the material surface are locally deviated from the microscope aperture, and the image at that point is dark. The strand is viewed as an otherwise clear object surrounded by dark outlines. The laser beam is drawn so that the end of the strand is in the center of the field of view, while the other end is anchored to the wall of the reservoir. The laser draw endpoint is fixed in space relative to the apparatus. The reservoir contains an engraved scale, marked in intervals of 0.05 inch to provide a length calibration in the bottom of the video image. Experiments are performed at initial strand lengths of 0.5, 1.0, and 1.5 inches. A typical view of a strand during shrinkage obtained using the Schlieren method is shown in Figure 8.

The recorded video tape is analyzed frame-by-frame to get shrinkage of the strand as a function of elapsed time. Measurements are made at intervals of 1/30 s for the first second of strand cure, and at progressively less frequent intervals, down to one frame every 10 s at 120 s elapsed time after the strand is drawn.

Initial shrinkage measurements were made by tracking the tip of drawn strands. The tips of 0.5 inch long strands tended to sink into the resin pool, making it impossible to accurately follow the tip shrinkage. Also, in some instances, unacceptable time intervals had to elapse after the laser draw before sufficient optical differences between the strand and the resin pool produced a

measurable video image. Acrylate shrinkage data was particularly difficult to reduce, regardless of strand length.

Because of the uncertainties in measuring the absolute tip position using the direct Schlieren method, an alternate method for measuring shrinkage was developed. In this method, a strand is drawn across the field of view to the microscope, and across a tag which floats on the surface of the resin. As the strand begins to shrink, it drags the tag along. Arts and crafts glitter, which has a fairly uniform size of about 0.020 inches square, was found to be an effective tag or float. Glitter is small, it floats, and it is highly reflective, making it very visible in the video. The lighting is adjusted to permit specular reflection from the glitter float into the camera, and also to permit viewing of the strand using the Schlieren approach. Figure 9 shows a glitter float image.

The glitter float method gave results for all three strand lengths, and proved to be more consistent than the direct Schlieren method. Linear shrinkage results, plotted as a function of elapsed time are given in Figures 10 and 11. For the single laser pass conditions of this study which measure the cure shrinkage of the gelled resin only, SL 5170 epoxy shrinks about 1.4% and SL 5149 acrylate shrinks about 1.0 percent. Shrinkage data are consistent for the three different strand lengths in the experiments. For the nominal 1.0 in/s draw velocity, linear shrinkage results are independent of strand length for lengths up to at least 1.5 inches. In this test method, no shrinkage is measured until the laser reaches the glitter and the strand attaches to it. The attachment must occur before strand shrinkage begins to move the float and shrinkage data is recorded.

University of Dayton Data

A contract was placed with the University of Dayton to perform complementary shrinkage experiments on both SL 5170 epoxy and SL 5149 acrylate resins. These linear shrinkage measurements were made using an optical microscope [6]. The 0.12 inch (3 mm) long strands in these tests were drawn with a full line laser exposure and the tests were not performed in situ inside stereolithography equipment. The University of Dayton's experimental program and strand shrinkage data are discussed in Appendix A.

FORCE MEASUREMENTS

Fixtures developed for in situ measurement of forces during cure shrinkage, step displacement loading, and stress relaxation tests of strands are schematically illustrated in Figure 12; a photograph of the fixture was shown earlier in Figure 3. A drawn strand attaches to tapered tabs that are just below the resin surface; one tab is connected to an extension from a miniature force gage and the other tab is connected to a platform whose movement can be controlled by an electronically-driven micrometer. Initial position of the platform is adjustable to permit testing of strands with different initial lengths; a 1.0 inch strand was used in all force tests. The 150 gram load force gage, calibrated to 20 grams full scale has a resolution of ± 0.02 gram. An LVDT (± 0.05 inch range) is used to monitor strand displacement imposed by the micrometer whose displacement rate and amplitude can be controlled. In all 0.5% step strain tests, strands are strained at a rate of about 0.01 s^{-1} .

In situ force tests are performed to measure (1) cure shrinkage forces that develop after single or multiple laser hits on single strand, (2) stress-strain response when a 0.5% step strain is imposed on a strand at different elapsed times after the strand is drawn, and (3) force-time relaxation response after 0.5% step strain. Initial modulus values are based on the initial slope of force-strain curves and the cross sectional area of the strand. These values of modulus are integrated averages over the strand cross section, whose properties are nonhomogeneous due to a cure gradient resulting from attenuation of laser energy in the resin. The cure gradient determines the extent of reaction (degree of cure) at different locations in the strand cross section.

SL 5149 acrylate data- A typical force versus time response of an SL 5149 acrylate strand which was hit with 4 laser exposures prior to applying 0.50% step strain is shown in Figure 13. This curve illustrates that no shrinkage forces are detected after the 1st laser hit, but that cure shrinkage forces are measured following additional laser hits. The actual linear shrinkage associated with multiple hits cannot be measured because the strands are attached at both ends and cannot shorten. The stress-strain responses during the 0.5% step strain provide initial modulus values.

Figure 14 clearly shows that the acrylate continues to shrink for at least 20 laser exposures. The magnitude of each additional cure shrinkage force increment decreases as the number of laser hits increases. A small region of Figure 14 is expanded in Figure 15 to show in greater detail the shape of the force-time response during and following a laser hit. It is of interest to note that immediately following a laser hit, the force initially decreases, possibly due to thermal expansion of the strand from laser heating. The strand then undergoes additional cure shrinkage producing a force that initially increases rapidly before leveling off.

Initial modulus of acrylate strands as a function of the number of laser hits is shown in Figure 16. The modulus calculations account for the strand area associated with the number of laser hits. Acrylate strands continue to shrink and to increase in modulus (degree of cure) following multiple laser hits, for at least 28 hits. This characteristic may be the primary reason that specimens built with SL 5149 acrylate have a greater tendency to curl than specimens built with SL 5170 epoxy. The initial modulus increases from about 1000 psi for a single hit to near 110,000 psi for a strand exposed to 28 laser hits. Recall that the strand is not recoated with fresh resin between laser exposures.

No shrinkage forces are detectable after a single laser draw. However, in 0.5% step strain tests, small forces were developed but the magnitude of these forces do not increase with elapsed time between the laser draw and application of the step strain. Figure 17 illustrates that the acrylates' initial modulus during the step strain appears to be almost independent of elapsed time following laser draw of the strand; initial modulus is 1000 to 2000 psi.

Following the application of the 0.5% step strain, the forces (stresses) relax with time in the manner shown in Figure 18. Recall that the area of a strand increases with additional laser hits. The representative curves shown in Figure 18 reflect the fact that the measured forces have been normalized to their respective areas.

SL 5170 epoxy data

Within the resolution of the force gage, no cure shrinkage forces were detected for SL 5170 epoxy strands after one laser pass. Any forces that developed during gelation and stiffening of the strand relaxed before they reached detectable levels. However, forces were measured when the strand was subjected to the 0.5% step strain. Strands were strained at different elapsed times following the laser draw. Initial stress-strain responses from tests with elapsed times up to 240 minutes show that both initial stiffness and peak force increase with longer elapsed times. Modulus values are plotted in Figure 17. These data, which are averages of three or more tests, illustrate the time dependence of initial modulus on elapsed time. The modulus continues to develop for times up to 240 minutes and begins to approach the manufacturer's reported 310,000 to 360,000 psi modulus for UV post cured specimens built with 3D Systems' WEAVE™ draw pattern.

In contrast to the acrylate resin, no shrinkage forces were detected for SL 5170 epoxy strands in tests in which specimens were subjected to as many as 8 laser hits. However, in tests on strands with multiple laser hits, initial modulus does not appear to be influenced by the number of hits but by the elapsed time from the 1st hit to the application of the step strain. Typical stress-strain responses for multiple hit strands are plotted in Figure 19. The stress-strain curves for 1, 2, and 3 laser hits are about identical (all with an elapsed time of 5 minutes). Strands with more hits and longer elapsed times had stiffer responses. Moduli data from these curves are compared with the single strike data as a function of elapsed time in Figure 20. These data seem to illustrate that the initial modulus SL 5170 epoxy is dependent on elapsed time and not the number of laser hits as is the SL 5149 acrylate.

Force relaxation responses after different elapsed times from laser exposure, before application of 0.5% step strain, are shown in Figures 21 and 22. Peak forces increase with longer elapsed times. Relaxation is recorded for times up to 800 s and with the possible exceptions of the 3 and 5 minutes elapsed time tests, the epoxy strands are still relaxing after the 800 s. Relaxation times increase with longer elapsed times.

BULK MATERIAL MEASUREMENTS

To this point, the in situ response of single strands to mechanical loading has been discussed. Additional tests were performed on strand and bulk specimens of SL 5170 epoxy. Single strands were drawn in the SLA-250 apparatus, removed after 5 minutes, cured in an ultraviolet (UV) chamber, then loaded in tension in an Instron test frame. Bulk material dogbone specimens (2.0 inches long by 0.32 inch wide by 0.29 inch thick gage section) were built in an SLA using the Accurate Clear Epoxy Solid (ACES™) build style [6], then cured in the UV chamber prior to tension testing in an Instron machine. In addition, ultrasonic wave speed measurements were made in the three principal orthogonal directions on cubic specimens built with the ACES™ build pattern and cured for 1 hour in a UV chamber. Results from these tests are reported in APPENDIX B. It is of particular interest to report that according to the ultrasonic measurements, multi-layered bulk material specimens built by standard stereolithography processes are isotropic. That is, the ultrasonic elastic moduli are identical in the three principal directions.

CURL MEASUREMENTS

Cantilever beam artifacts of the dimensions shown in Figure 23 were built and the resulting out-of-plane curl was measured. Figure 24 illustrates the two different laser beam vector paths (build styles) used to build the specimens. In one build style, the direction of the laser is always in the 1-(length-wise) direction of the cantilever. In the other build style, the laser path primarily utilizes vectors in the 2- (transverse) direction of the cantilever. A 0.010 inch resin recoat is applied for each layer; the center section of the specimen is 5 layers thick and the cantilever beam is 4 layers thick. Each strand in the cantilever beams was drawn with one laser exposure and allowed to fully react before being subjected to a second exposure. During the build, the second exposure occurred only after allowing time for the reaction from the first exposure to come to completion.

In the Style I longitudinal build (see Figure 24a), vector paths 1, 2, and 3 were drawn (exposure 1), followed by a 200 second delay and then a second laser exposure. The programmed delay between build layers during the recoating operation was likewise about 200 seconds. In the transverse build style of Style II, the procedure to doubly expose each layer was more complicated. The base and first layer of the overhang in the cantilever were drawn using longitudinal vectors as in Style I to provide a support for the transverse vectors in the remaining layers. Without a lower layer for attachment, these short vectors would drift away in the resin vat before they could be struck a second time. The procedure for constructing the transverse vectors in the subsequent layers is described as follows using the 5 vectors in Figure 24b as an example:

1. Expose transverse vectors 1, 2, 3, and then wait about 200 seconds for these vectors to react (solidifying and shrinking).
2. Fill in the gaps between these vectors by drawing vectors 4 and 5 and then wait another 200 seconds for these vector strands to cure.
3. Expose vectors 1, 2, and 3 for a second time and then wait another 200 seconds.
4. Expose the in-between vectors, 4 and 5, and then wait 200 seconds.
5. Move on to next layer repeating the process after recoating.

In the actual beam, substantially more vectors were required to achieve the necessary length. However, the procedure for exposing alternate transverse vectors, waiting for the reaction to terminate, and then exposing the in-between vectors remains the same.

After cantilever beams of each style were built, they were removed from the SLA-250 for curl measurements (the specimens were not cured in a UV chamber). A side view of each specimen was photographed using an optical microscope; a typical specimen of each build style is shown in Figure 25. The photographs were digitized and image analysis software was used to measure the out-of-plane (3-direction) curl or distortion. The curves in Figure 26 shows typical beam curl as a function of relative position along the cantilever. The data are presented as a function of relative position along cantilever because rounding of its bottom edge at the beam support makes it impossible to precisely define its origin. There is slightly more curl in the transverse Build Style II cantilever specimen than in the longitudinal Build Style I beam.

The curl measured in the solidified parts was compared to model predictions obtained by analyzing the two build styles in a 3D finite element code [3]. The finite element program contained three important build features: 1) time varying material behavior; 2) laser path

dependence, scanning rate, and depth of cure; and 3) structural linkage. The finite element program also utilized a phenomenological material model of the solidifying resin. The material model is based on the cure shrinkage and stress relaxation data reported here. Qualitative agreement between analysis and experimental values was found in both the degree of curl and distinction between build styles.

SUMMARY

- New techniques were developed and used to make in situ property measurements of gelled resin to determine linear shrinkage, stress-strain response and stress relaxation of single strands of SL 5170 epoxy and SL 5149 acrylate ester photocurable resins. In a single laser exposure, epoxy strands shrank approximately 1.5% and the acrylate strands about 1.0%. No cure shrinkage forces were measured after the first laser hit in either epoxy or acrylate, and none was measured after multiple laser hits in the epoxy. This suggests that the epoxy either does not continue to shrink after the first hit or that shrinkage forces cannot overcome strand stiffness. On the other hand, the acrylate develops additional cure shrinkage forces for 20 or more laser hits. In force relaxation tests, a strand is drawn and then a 0.5% step strain is applied after a different number of laser hits and/or elapsed time between the first hit and the step strain. The acrylate initial modulus is a function of the number of laser hits, but not the elapsed time. In contrast, epoxy modulus is a function of elapsed time, but not the number of laser hits.
- Metallographic procedures were also developed and used to examine cross-sections of resin strands. The cross sectional area of strands increased with additional laser hits (no recoating with liquid resin between hits). The increase in area with laser hits was greater for the epoxy than for the acrylate.
- Procedures were developed to measure out-of-plane distortion (curl) of cantilever beam specimens built by two different build styles. Qualitative agreement between analysis and experimental values was found in both the degree of curl and distinction between build styles.
- Appendix A contains strand linear shrinkage data generated by the University of Dayton, on contract to Sandia National Laboratories. Appendix B reports on the tensile stress-stress response of UV cured strands, and tensile and ultrasonic properties of multi-layered specimens. And Appendix C lists some LDRD project related information.

REFERENCES

- [1]. SLA-250 User Guide, 3D Systems, Inc., April 1991.
- [2]. Chambers, R. S., Guess, T. R., and Hinnerichs, T. D., "*A Phenomenological Finite Element Model of Part Building in the Stereolithography Process*," Proceedings of the Sixth International Conference on Rapid Prototyping, June. 4-7, 1995, Dayton, Ohio.
- [3]. Chambers, R. S., Guess, T. R., and Hinnerichs, T. D., "*A Phenomenological Finite Element Model of Stereolithography Processing*," Sandia National Laboratories Report SAND96-0287, February 1996.
- [4]. Guess, T. R., Chambers, R. S., Hinnerichs, T. D., McCarty, G. D., and Shagam, R. N., "*Epoxy and Acrylate Stereolithography Resins: In-Situ Measurements of Cure Shrinkage and Stress Relaxation*", Proceeding of the Sixth International Conference on Rapid Prototyping, Dayton, Ohio, June 1995.
- [5]. Guess, T. R., and Chambers, R. S., "*In-Situ Property Measurements on Laser-Drawn Strands of SL 5170 Epoxy and SL 5149 Acrylate*", Proceeding of the Sixth Solid Freeform Fabrication Symposium, Austin, Texas, August 1995.
- [6]. Maestro Workstation User Guide for Software Release 1.7, 3D Systems Corporation, July 1995, pp. 2-23 to 2-25.

ACKNOWLEDGMENTS

This work was performed at Sandia National Laboratories and supported by the US Department of Energy under contract DE-AC04-94AL85000. Gerald McCarty, Brian Pardo, Daryl Reckaway and Mark Enszt operated the SLA-250 equipment, drew the strands and performed the force relaxation tests. Dale McGuffin prepared the metallographic samples and made the area and curl measurements. Lane Harwell and Carl Leishman developed the data acquisition software. Pete Stromberg designed the fixturing for in situ stress relaxation tests. Mark Stavig assisted in instrumentation selection and calibration and performed mechanical property tests on bulk material. Clint Atwood provided stereolithography technical support and, along with Doug Adolf, reviewed this report. John Gieske conducted the ultrasonic measurements. Richard Chartoff, Jill Ullett, and A. J. Lightman at the University of Dayton assisted in making property measurements and provided SLA software that allowed us to create our own build styles. Manfred Hofman at Ciba-Geigy and Paul Jacobs at 3D Systems discussed issues and reviewed SLA technology with us.

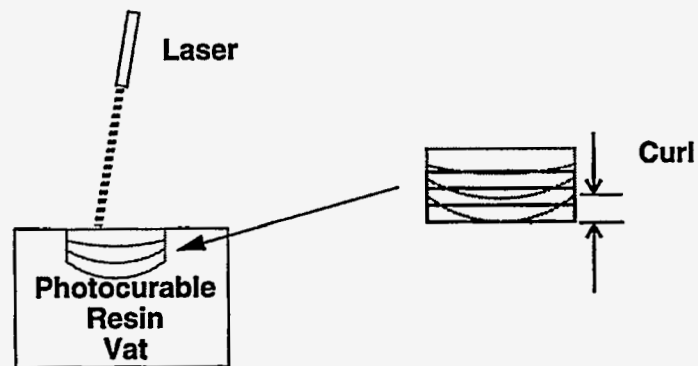


Figure 1. Schematic of stereolithography process

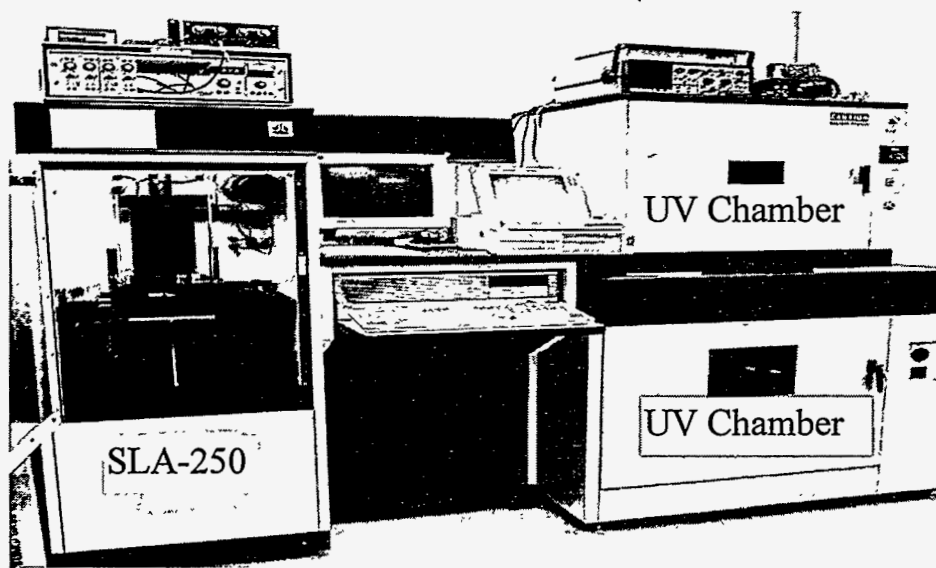


Figure 2. 3D System's SLA-250 stereolithography apparatus with the door open showing location of force measuring fixture. Post curing chambers are on the right.

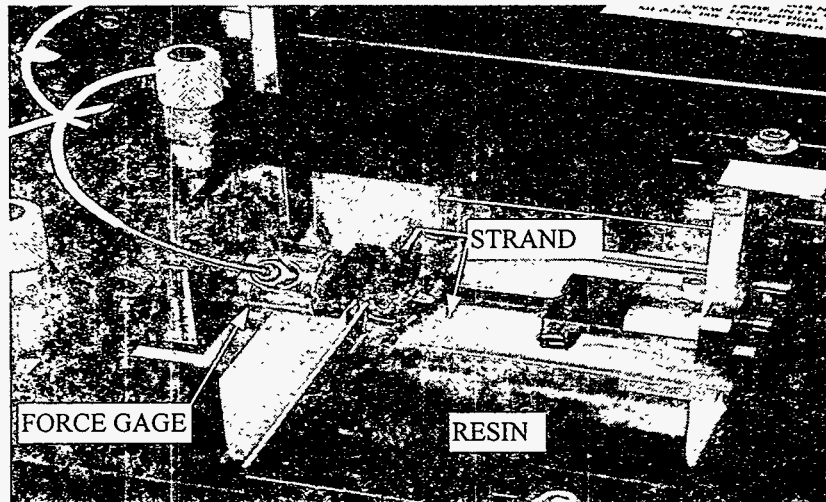


Figure 3. Expanded view of the force measuring fixture.

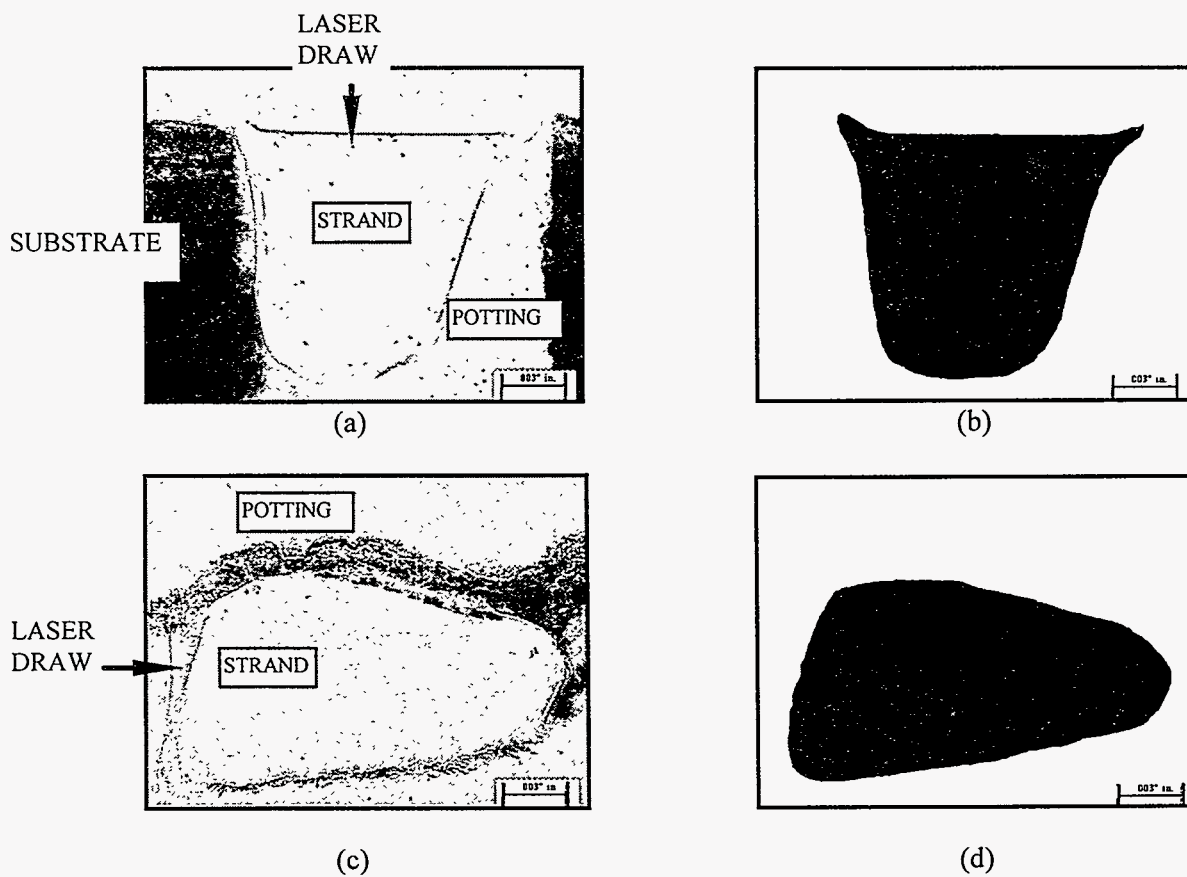


Figure 4. Typical cross sections of strands drawn with a single pass of a HeCd laser: (a) dark field image and b) binary image of SL 5170 epoxy; and (c) dark field image and d) binary image of SL 5149 acrylate. A scale marker of 0.003 inch length is shown in each image.

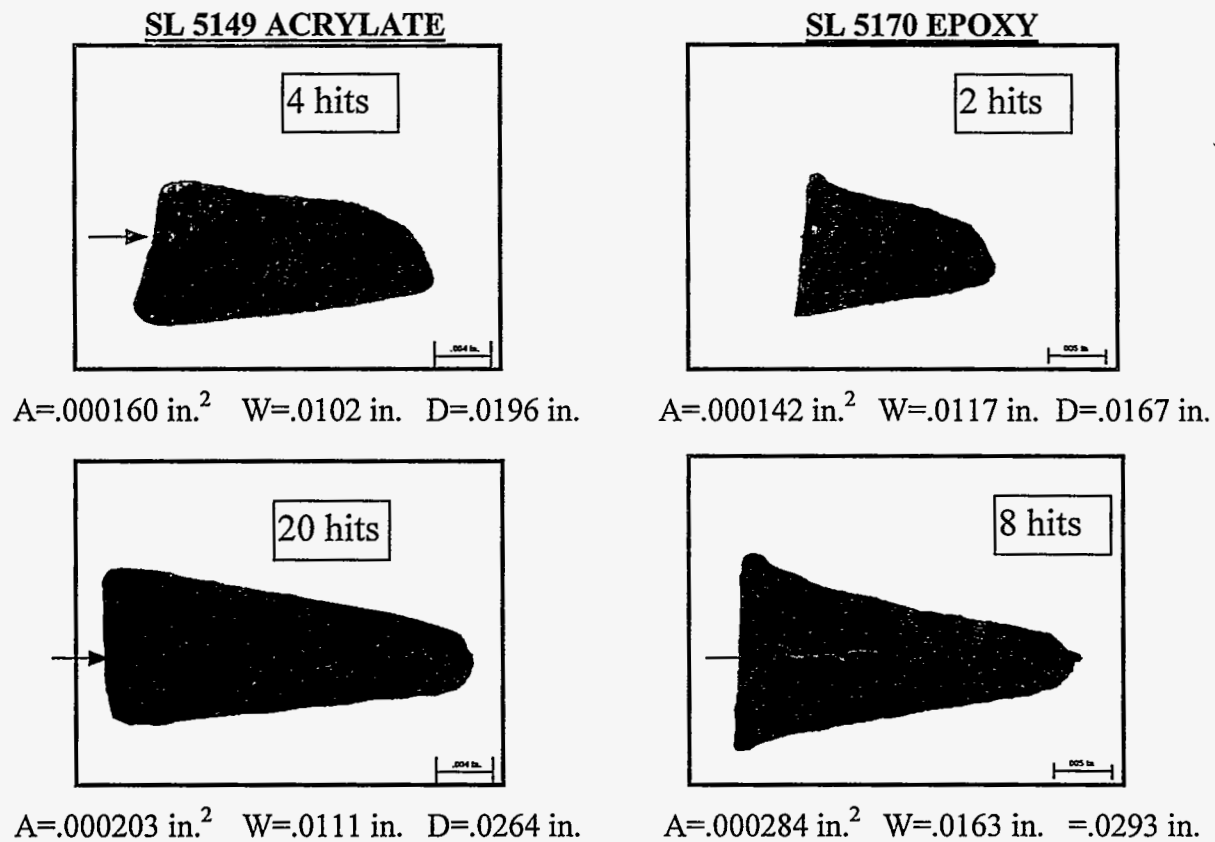


Figure 5. Cross sections of SL 5149 acrylate and SL 5170 epoxy strands for different number of laser hits. Arrow indicates direction of laser hit. Strands were not recoated between hits. A, W and D denote strand area, width (at widest point) and depth, respectively. A scale marker of 0.004 inch length is shown for each acrylate image and a 0.005 inch marker for each epoxy image.

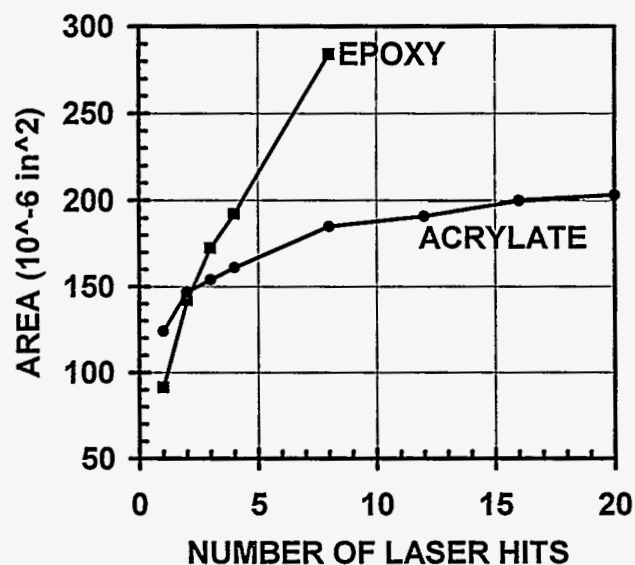


Figure 6. Strand cross sectional area as a function of number of laser hits.

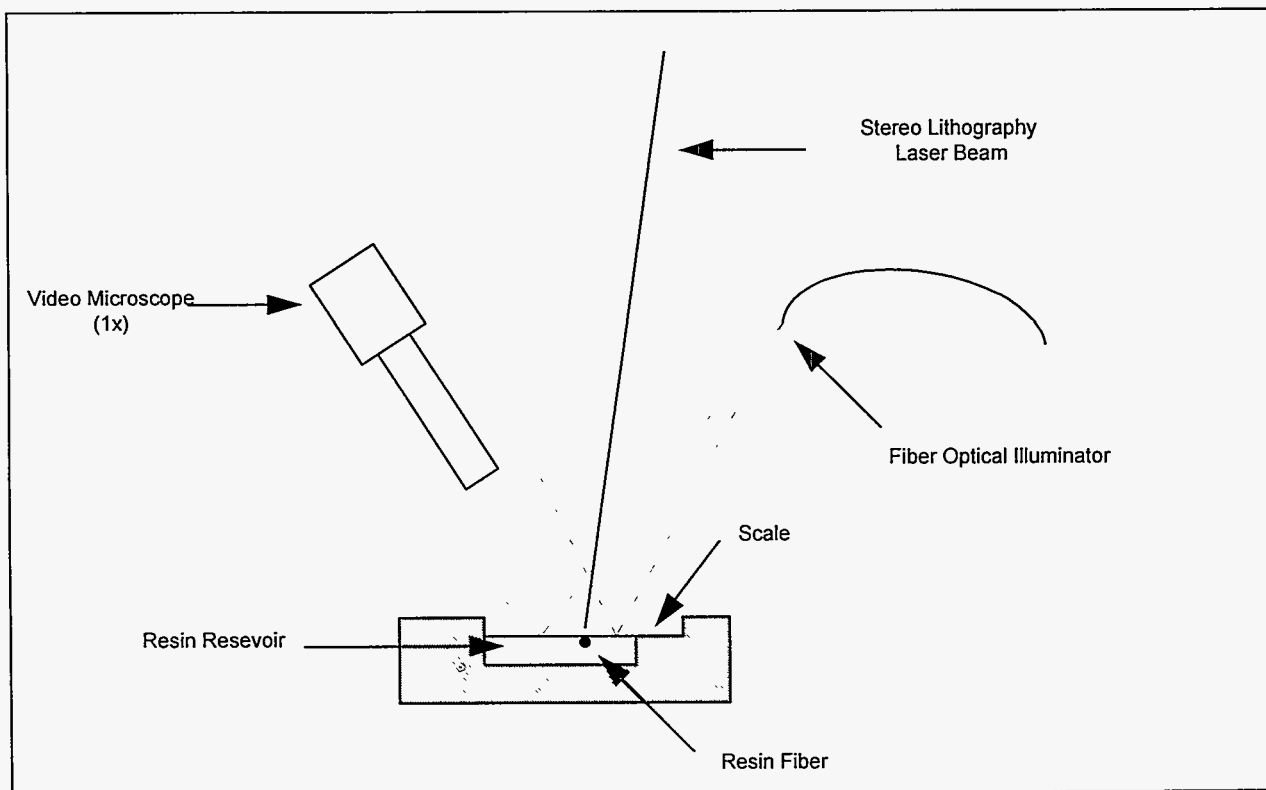


Figure 7: Schematic of setup for video measurement of strand linear shrinkage.

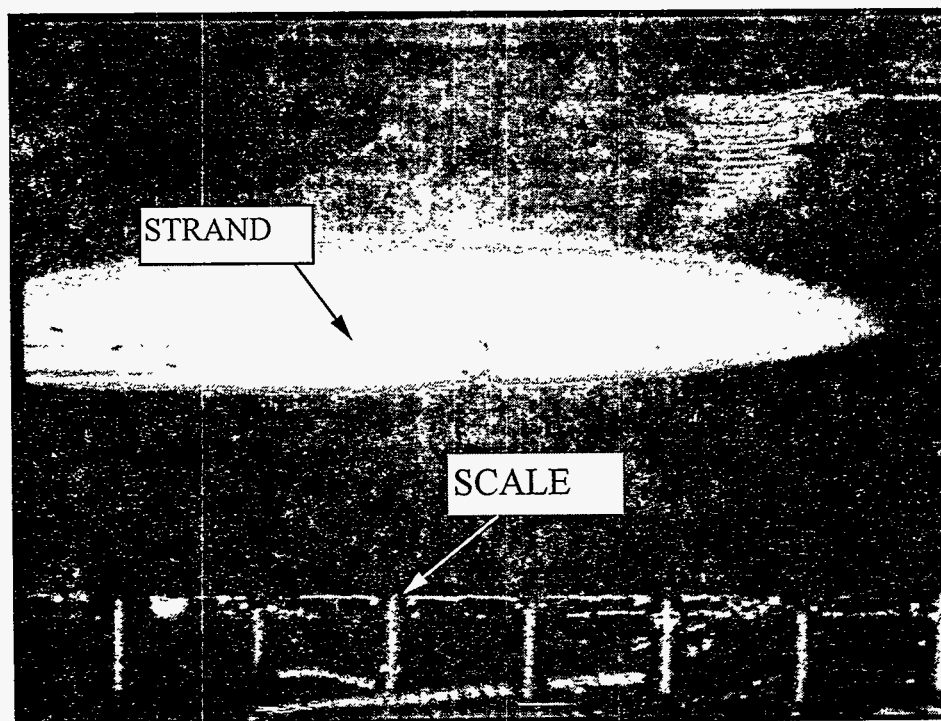


Figure 8. View of strand tip using Schlieren method.

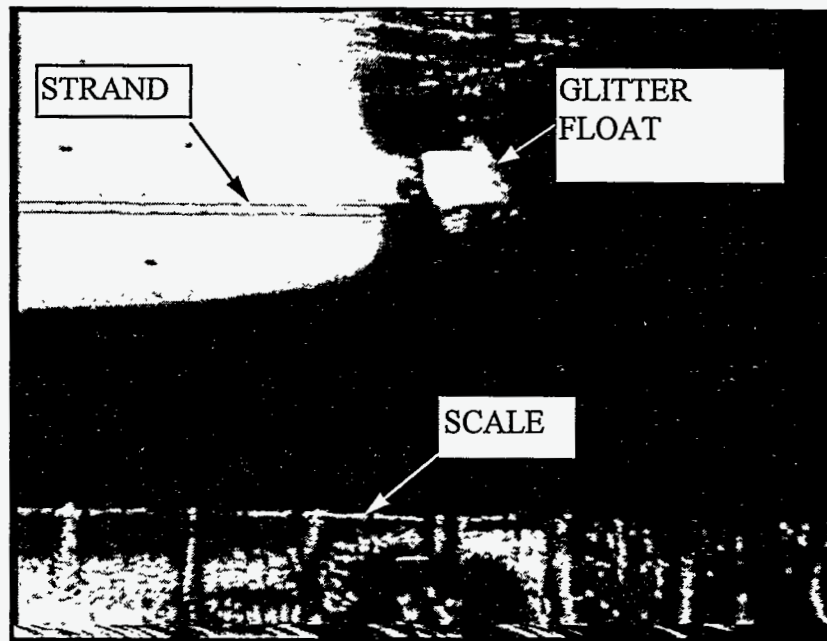


Figure 9: View of strand and tag using the glitter float method.

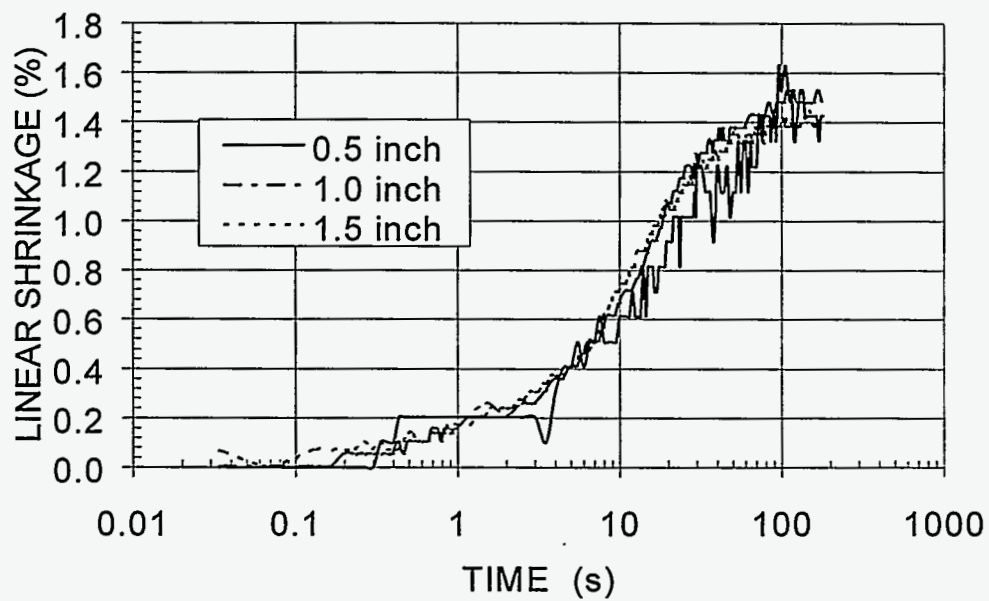


Figure 10. Linear shrinkage of SL 5170 epoxy: comparison of results from three different lengths of strands drawn in an SLA-250 stereolithography machine.

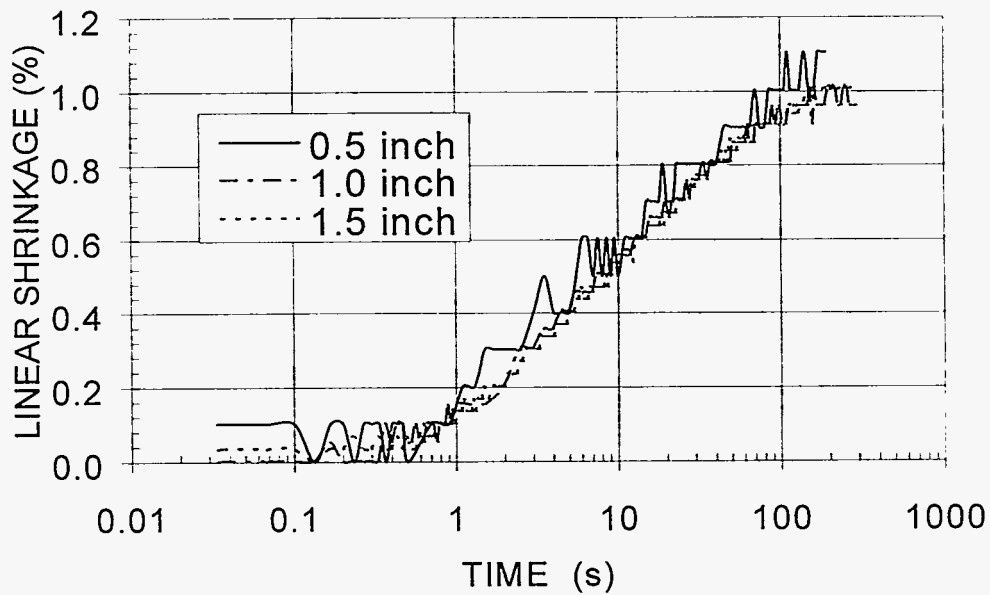


Figure 11. Linear shrinkage of SL 5149 acrylate: comparison of results from three different lengths of strands drawn in an SLA-250 stereolithography machine.

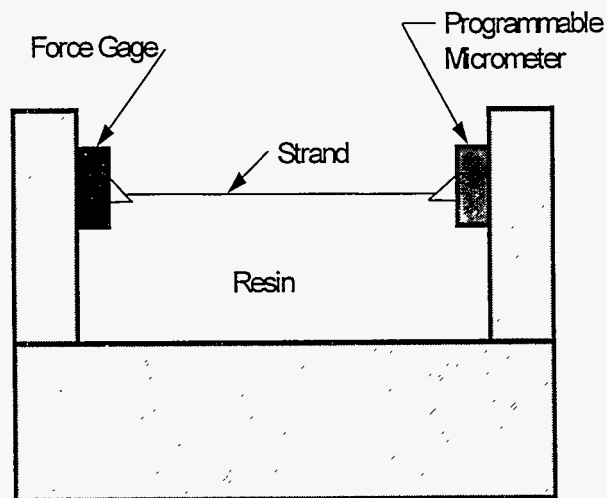


Figure 12. Schematic of experimental setup for force measurements and stress relaxation experiments.

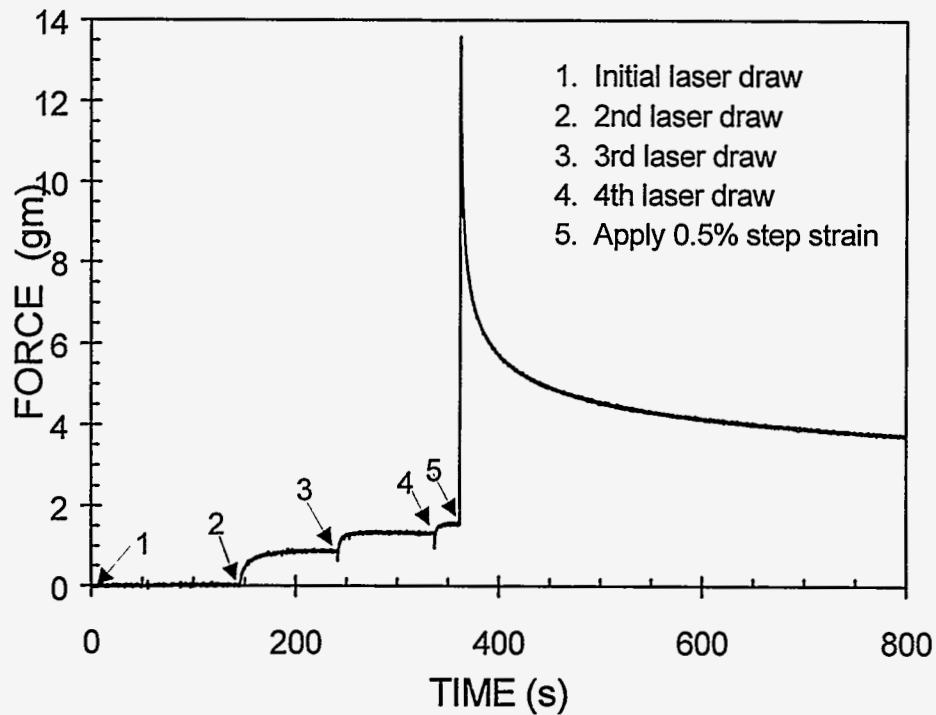


Figure 13. Forces developed in SL 5149 acrylate due to multiple hits of the laser and a 0.5% step strain to a 1.0 inch strand. Force relaxation occurs following the step strain.

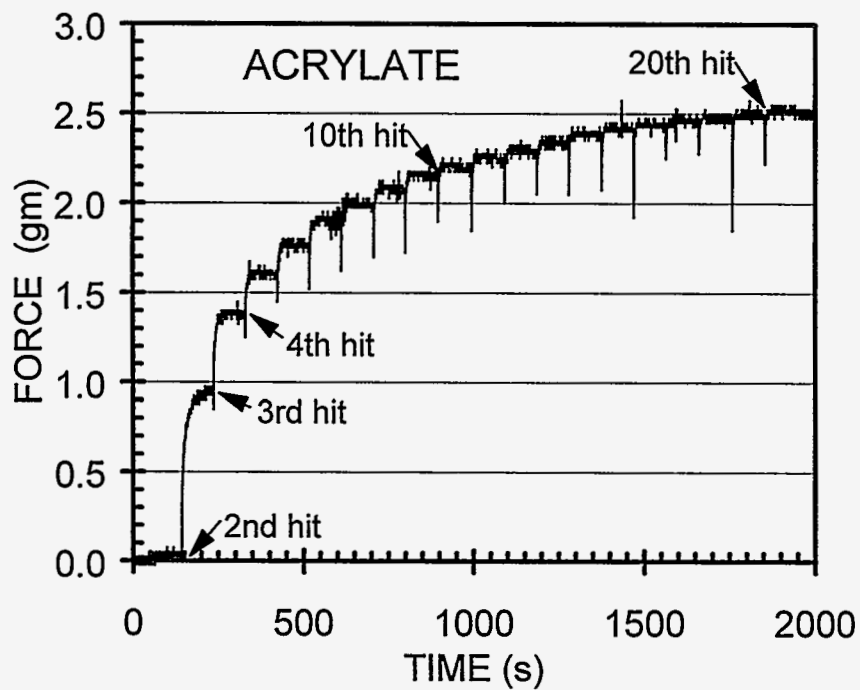


Figure 14. Cure shrinkage forces in a 1.0 inch acrylate strand due to multiple hits of the laser.

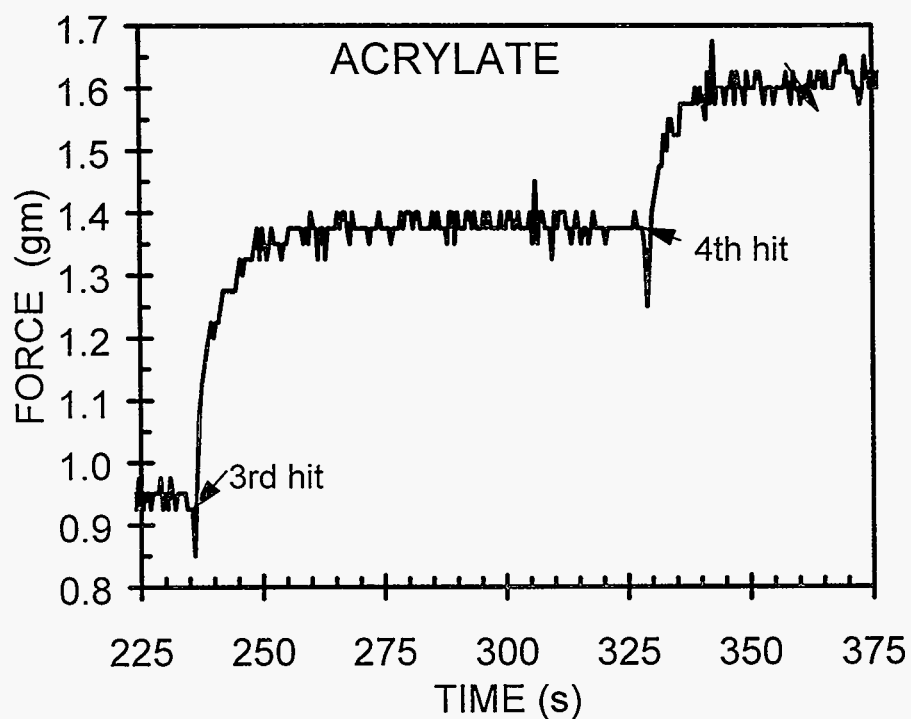


Figure 15. Expanded view of cure shrinkage forces in the Figure 14 acrylate strand.

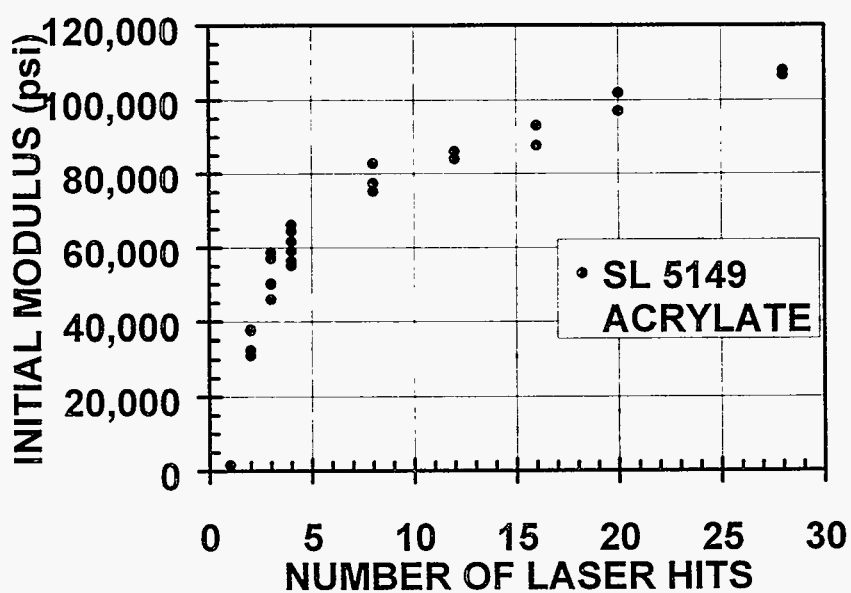


Figure 16. Initial modulus of SL 5149 acrylate as function of number of laser hits.

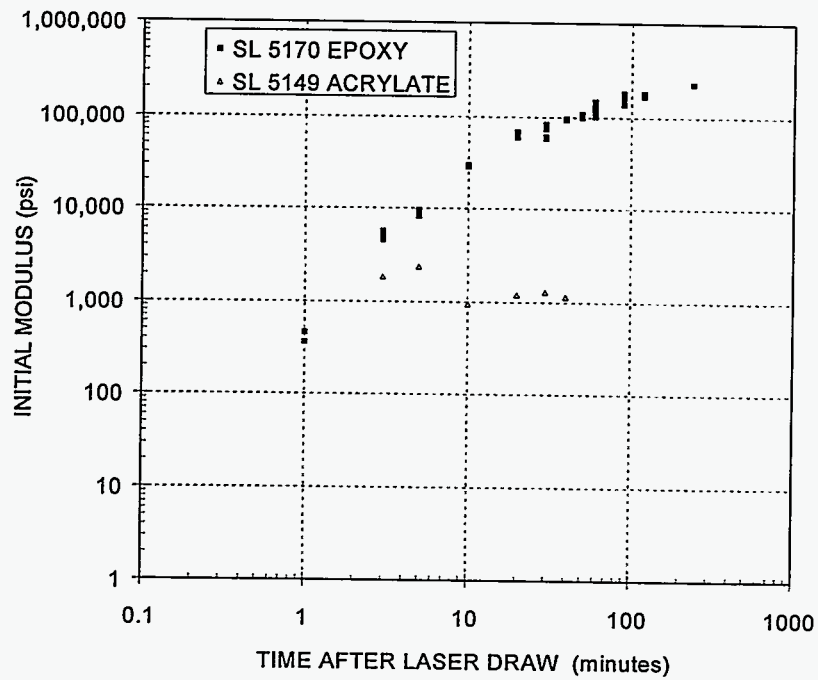


Figure 17. Initial modulus of SL 5170 epoxy and SL 5149 acrylate as a function of time following the laser draw of a strand. The strand remains in the resin vat during the time interval between the draw and the tensile test.

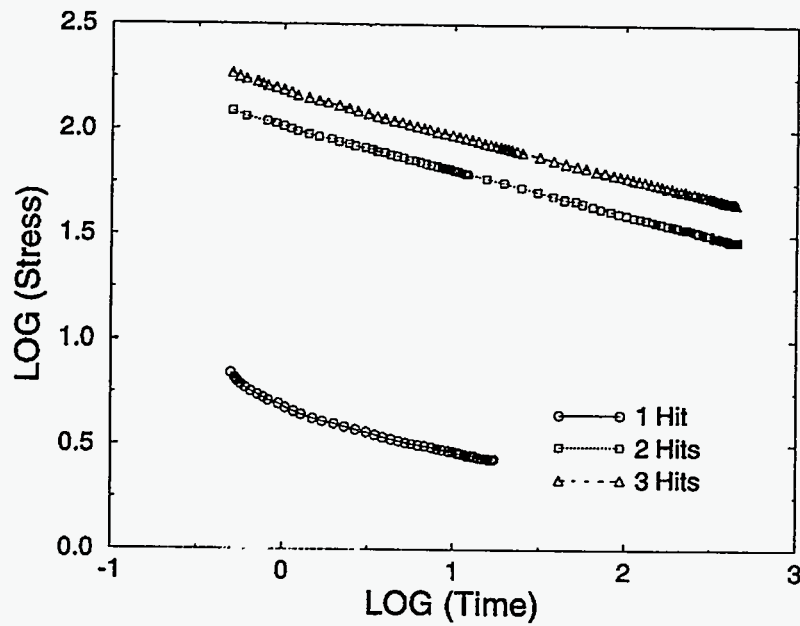


Figure 18. Stress relaxation measured in single strands of SL 5149 acrylate resin following multiple laser hits (stress in psi and time in seconds).

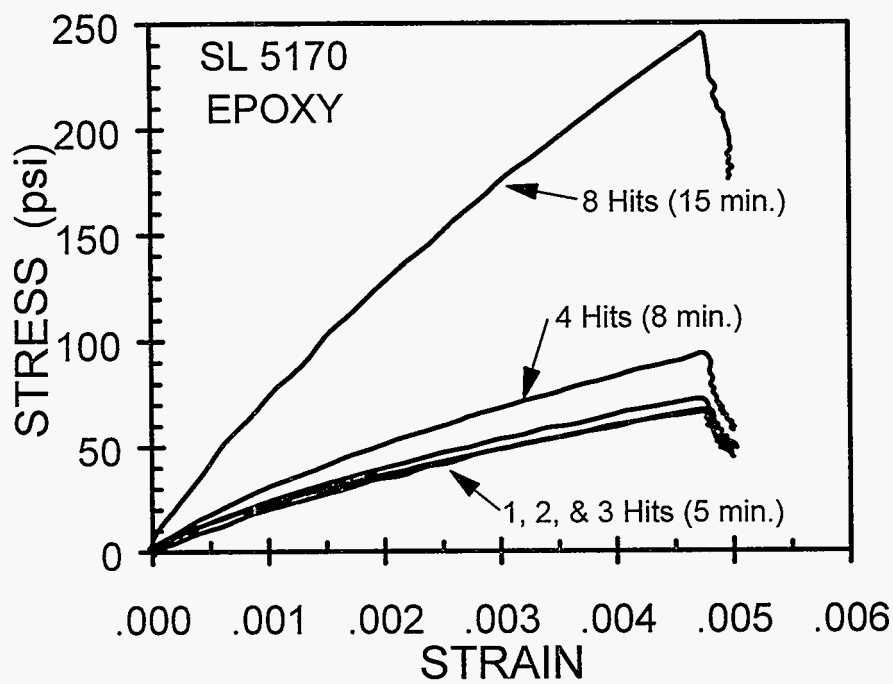


Figure 19. Stress vs. strain response of SL 5170 epoxy strands for different number of laser hits.

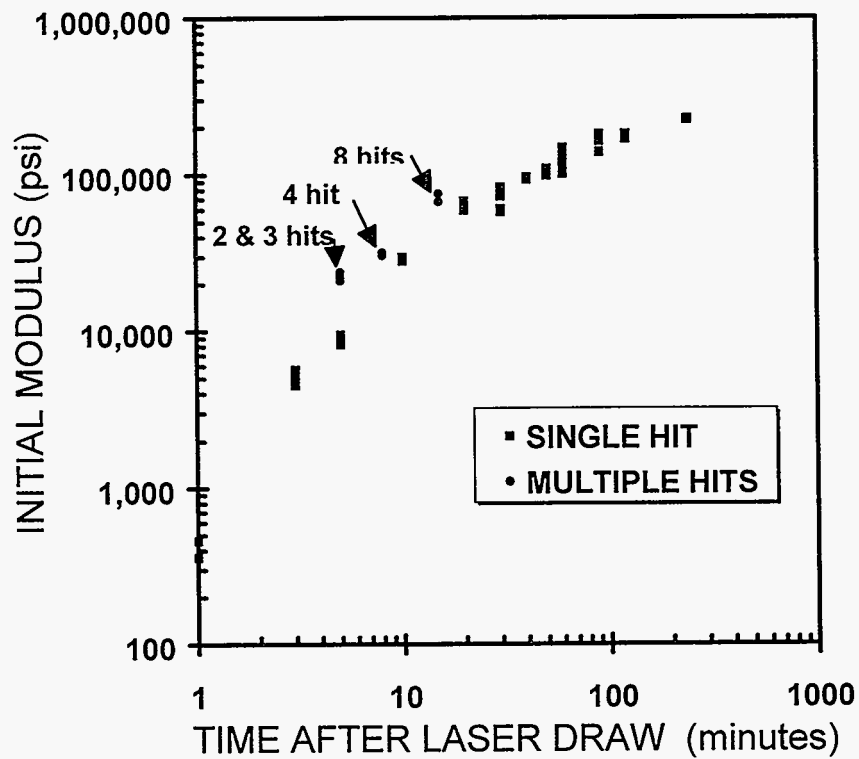


Figure 20. Initial modulus of SL 5170 epoxy strands as a function of elapsed time from the 1st laser hit.

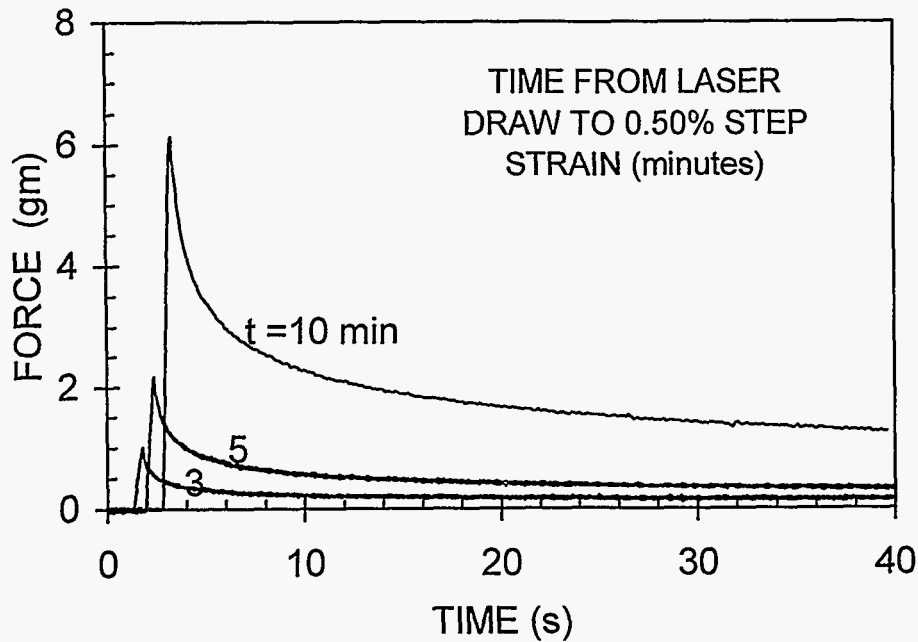


Figure 21. Force relaxation of SL 5170 epoxy. Step strain of 0.5% applied to strand at different times following the laser draw of a strand. The strand remains in the resin vat during the time interval between the draw and the tensile force relaxation test.

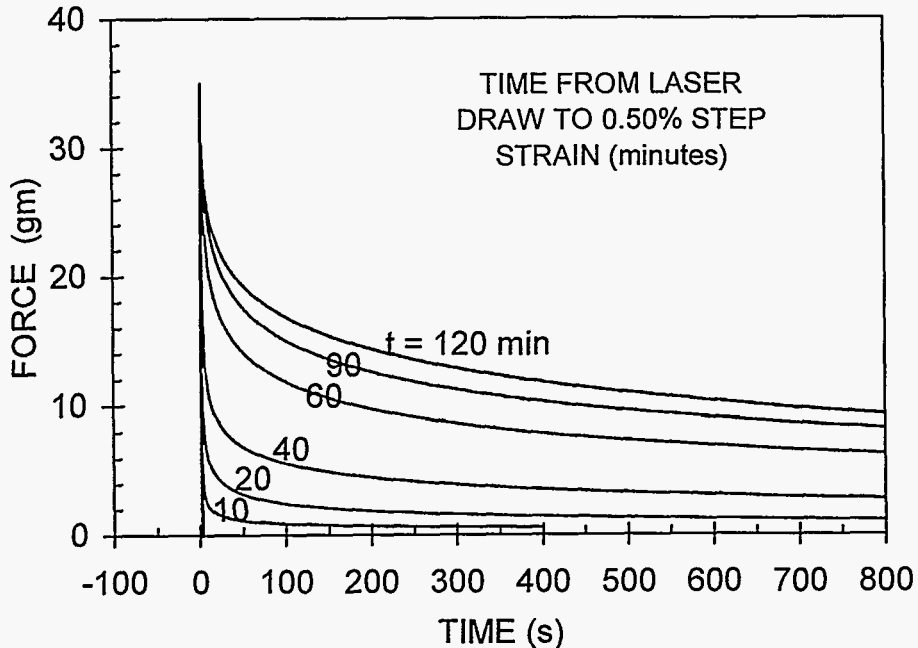


Figure 22. Force relaxation of SL 5170 epoxy. Step strain of 0.5% applied to strand at different times following the laser draw of a strand. The strand remains in the resin vat during the time interval between the draw and the tensile force relaxation test.

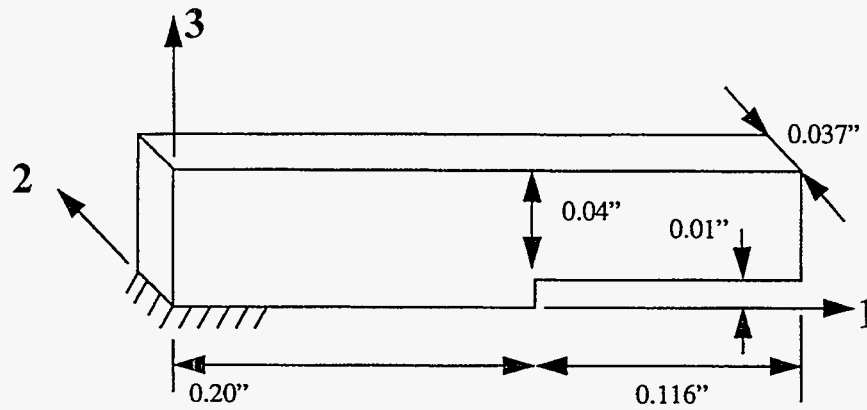


Figure 23. Dimensions (inches) of SL 5149 acrylate cantilever beam specimen for distortion (curl) measurements.

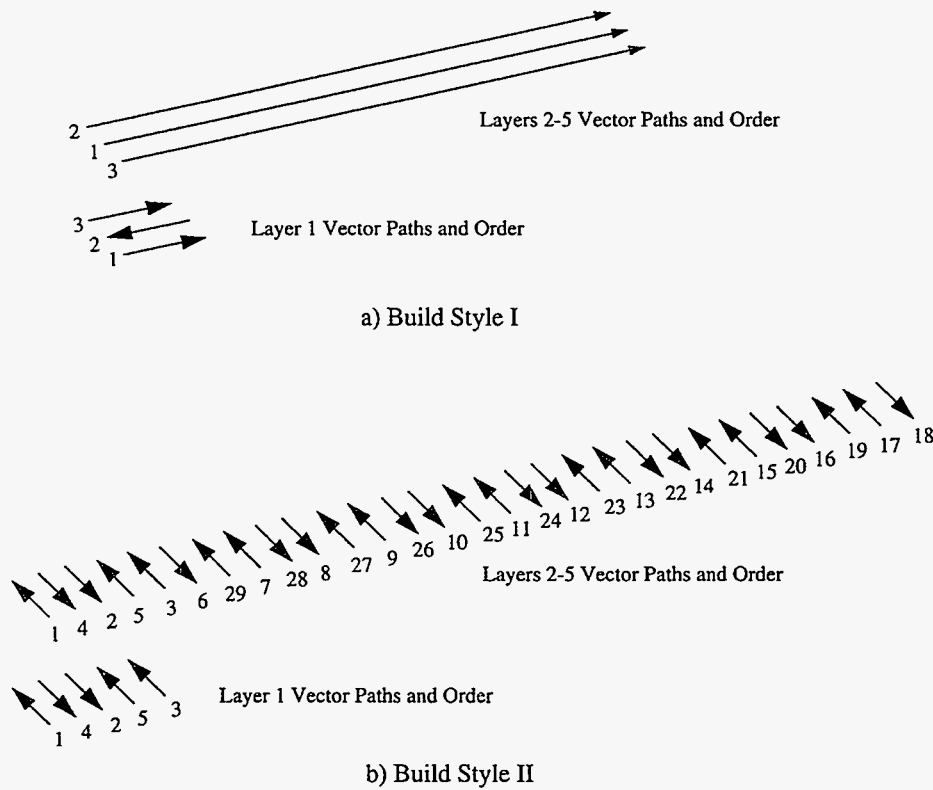
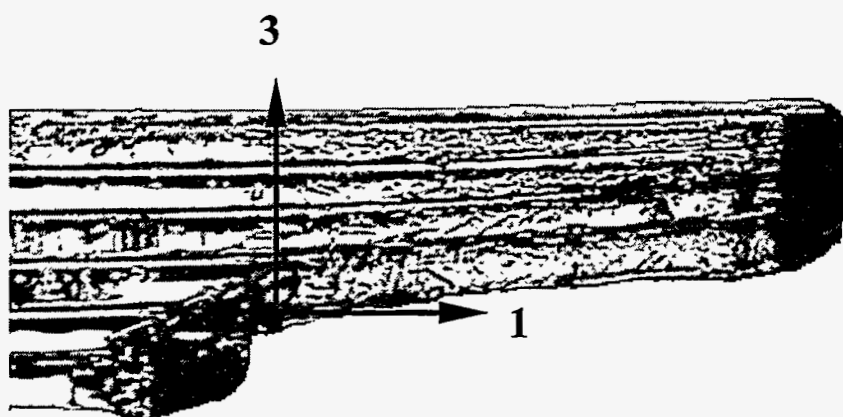
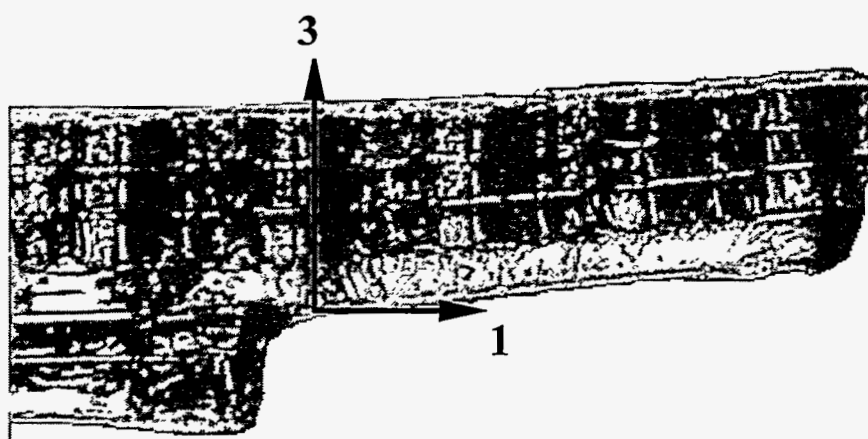


Figure 24. Schematics illustrating the vector paths and drawing sequence for the two build styles curl measurement specimens. Analysis of the cantilever beams and comparison between experiment and calculations are discussed in Reference [3].

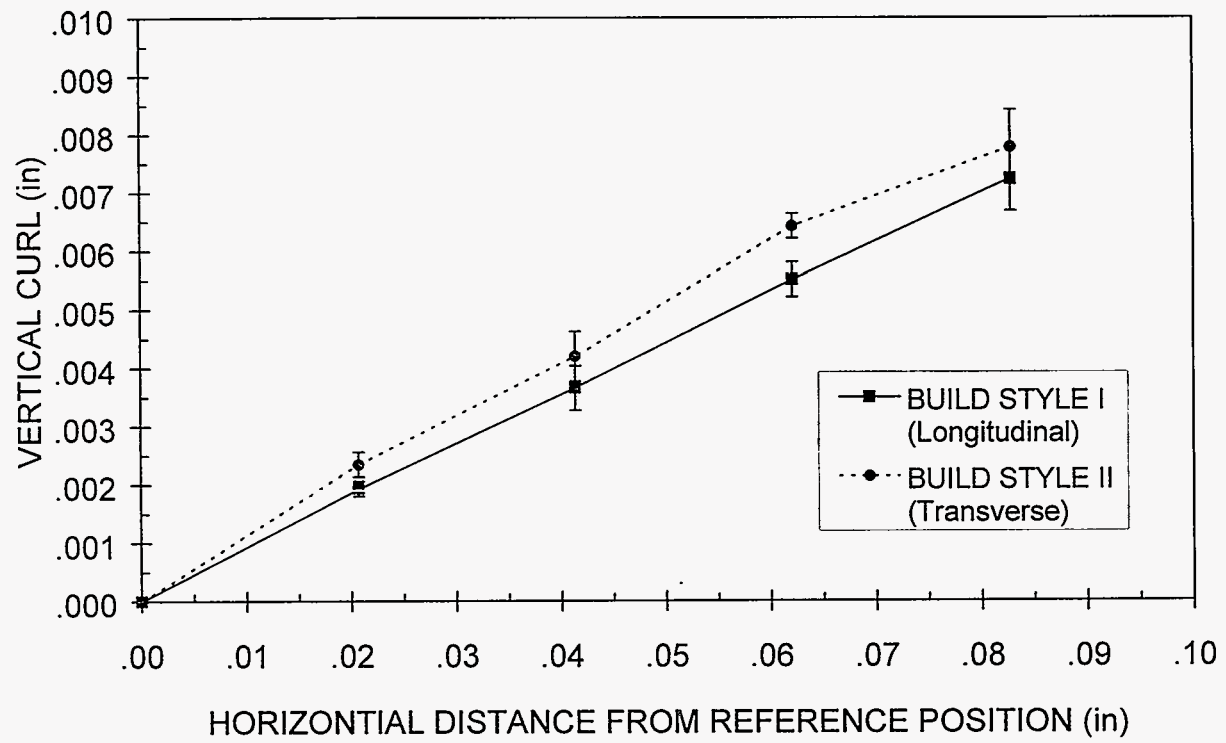


(a)



(b)

Figure 25. Representative picture of SL 5149 acrylate cantilever beams from the two build styles, the beams were not post cured: (a) Build Style I cantilever beam and (b) Build Style II cantilever beam.



(c)

Figure 26. Measured out-of plane curl of SL 5149 acrylate Build Style I and Build Style II cantilever beams.

APPENDIX A

University of Dayton Cure Shrinkage Data

Dr. Richard Chartoff, Professor of Materials Engineering and Head of Basic and Applied Polymer Research at The University of Dayton has been studying stereolithographic processes and the relevant photocurable resins for about five years. He and his staff have examined the reaction kinetics and have proposed models for predicting the extent of reaction and exotherms generated during curing. Staff at The University of Dayton have also measured linear shrinkage during curing and written special software for the SLA-250 stereolithography equipment to provide addition controls for pattern drawing. Because Dr. Richard Chartoff and his associates have an expertise in the photocurable resin systems, a \$35k contract was placed to enlist their support. The contractual statement of work included the task of making linear shrinkage measurements on SL 5170 epoxy resin and SL 5149 acrylate resin.

The following information from progress reports sent by Dr. Jill Ullett of the University of Dayton and is presented without additional comment.

LINEAR SHRINKAGE MEASUREMENTS

The test set-up consists of a small vat which is temperature controlled and contains a small shelf upon which one end of a sample is eventually attached. A laser draws a single strand specimen, approximately 3 millimeters long from the vat shelf to the sensing arm of a primary balance. As the sample shrinks, it pulls the primary balance sensing arm which in turn causes the leverage arm to push a secondary balance arm. During this motion, a mirror chip rotates and deflects the beam from a second laser which is directed to a meter stick along a perpendicular path. Gradations along the meter stick are calibrated to the motion of the strand, and the history of change is video-recorded for later data reduction. The system has been calibrated and used to generate data on at least a couple different resin systems.

Prior to testing every data set, the linear shrinkage apparatus (Figure A1) was calibrated. A micrometer driven translation stage was used to move the balance arm through full scale deflection. The change in position of the HeNe probe beam with stage position was recorded. The calibration data were plotted and a least squares fit used to obtain a linear expression for the slope of the data; the slope is the calibration factor of the system.

Data Set #1: SL 5170 Epoxy-- 2 exposures with 5 minutes delay between exposures.

Four linear shrinkage trials were conducted using the SL 5170 epoxy resin in the single-balance shrinkage apparatus. The test conditions are summarized in Table A1. In each trial the resin was exposed for 30 milliseconds to the HeCd laser which had a measured power output (at the vat) of 16 milliwatts. Shrinkage data were recorded for 5 minutes at which time a second 30 millisecond exposure was made. Data were then recorded for another 5 minutes. A second

strand was made using a single 30 millisecond exposure so that cure depth after a single exposure could be measured. All strand cure depth measurements were made using an optical microscope. Key data are summarized in Table A2.

Cure depth measured after the first exposure was uniformly about 76% of the final cure depth. Cure depth increased from an average of 0.20 mm (0.008 inch) for the first exposure to 0.26 mm (0.010 inch) measured 5 minutes after the second exposure. Shrinkage, however, did not increase with the second exposure. The average final shrinkage for the four trials was 1.24% with a standard deviation of 0.147 (1.2%). A plot of the average shrinkage as a function of time is given in Figure A2.

Data Set #2: SL 5149-Acrylate-- 2 exposures with 5 minutes, 10 minutes, or 1 second delay between exposures.

Initial shrinkage trials with the SL 5149 acrylate resin indicated that after an initial 10 ms exposure from the HeCd laser (power at the vat was 16 mW) the shrinkage leveled off and then decreased before a second 10 ms exposure was made at an elapsed time of 300s (5 minutes). After the second exposure, the shrinkage increased rapidly past the maximum observed for the first exposure. Data for one trial are shown graphically in Figure A3. Two questions were then posed: What happens to the shrinkage if the wait between exposures is extended from 5 to 10 minutes, and what is the change in cure depth from one exposure to two?

In response to the first question a trial was made using a 10-minute wait between 10 ms exposures. Figure A4 shows the results graphically. At an elapsed time of about 27 seconds the shrinkage reached a plateau of 0.568%. At an elapsed time of 77 seconds the shrinkage began to decline. A minimum value of 0.074% was measured at an elapsed time of 634 seconds at which time the second exposure was made. The shrinkage then increased to a value of 0.962% at an elapsed time of 686 seconds and then began to decrease. The experiment was terminated before a constant shrinkage value was reached.

Cure Depth Data

Cure depth values for singly exposed and doubly exposed strands were measured under several sets of conditions. (Shrinkage data were not recorded for these experiments.) The laser power measured at the vat was 16 mW for all trials. Results are summarized in Table A3.

Trials with 1-Second Delay Between Exposures

A set of three linear shrinkage trials was made with the SL 5149 acrylate resin using 10 ms exposures with a 1.0 second delay between exposures. The conditions for these trials are given in Table A4 and the results are summarized in Table A5. The average response from the three trials is plotted and summarized in Figures A5. The average final shrinkage measured was 1.34% with a standard deviation of 0.021. This shrinkage value is considerably higher than the maximum value (0.96%) recorded for the trial in which there was a 10 minute wait between exposures. The average final cure depth for the three trials was 0.306 mm (12 mil). This value is

larger than all values measured (see Table A3) for trials in which there was a 5 minute delay between exposures.

Table A1. Test Conditions for SL 5170 Trials- Data Set #1

Vat temperature = 30°C
 Ambient temperature = 22.2°C
 Relative humidity at 22.2°C = 35%
 Laser power at vat = 16 mW
 Exposure time = 30 ms
 Number of exposures = 2
 Delay time between the two exposures = 300s
 Strand length = 3 mm

Table A2. Summary of SL 5170 Linear Shrinkage Measurements- Data Set #1

	Trial 1	Trial 2	Trial 3	Trial 4	Average	Standard Deviation
Strand width (mm)	0.200	0.205	0.210	0.203	0.20	
Cure depth 5 min. after 1st exposure (mm)	0.199	0.204	0.201	---	0.20	
Final cure depth (mm)	0.260	0.268	0.262	0.260	0.26	
Final shrinkage (%)	1.218	1.233	1.250	1.247	1.240	0.147

Table A3. Cure Depth Measurements of SL 5149 Acrylate Resin

Trials	Number of Exposures	Exposure Time (ms)	Cure Depth (mm)	Comments
Data Set 1	1	10		Strands measured immediately after exposure
Trial 1			0.192	
Trial 2			0.195	
Trial 3			0.189	
Avg.			0.192	
Data Set 2	1	10		Strands measured after 5 min wait in vat after exposure
Trial 1			0.206	
Trial 2			0.227	
Trial 3			0.233	
Avg.			0.222	
Data Set 3	2	10, 10		Strands measured after 5 min wait in vat after 2nd exposure
Trial 1			0.237	
Trial 2			0.249	
Trial 3			0.248	
Avg.			0.244	
Data Set 4	2	10, 20		Strands measured after 5 min wait in vat after 2nd exposure
Trial 1			0.322	
Trial 2			0.303	
Trial 3			0.282	
Avg.			0.302	

Comments related to the Table A3 data are as follows:

- (1) In the first set of experiments, strands were exposed for 10 ms. The strands were immediately removed from the vat and measured. The average cure depth for this set of three trials was 0.192 mm (7.6 mil) with a standard deviation of 0.002 (1.2%).
- (2) In the second set of trials, the resin was exposed for 10 ms, left undisturbed in the vat for 5 minutes, and removed for measurement. The average cure depth for three trials was 0.222 mm (8.7 mil) with a standard deviation of 0.011 (5%).
- (3) In the third set of trials the resin was exposed for 10 ms, a 5-minute wait ensued, and a second 10 ms exposure was made. The strands were left undisturbed in the vat for 5 minutes, removed, and measured. The average cure depth for the three trials was 0.244 mm (9.6 mil) with a standard deviation of 0.005 (2%).
- (4) The final set of trials was similar to the third except that the second exposure was for 20 ms not 10 ms. The average cure depth measured for these trials was 0.302 mm (11.9 mil) with a standard deviation of 0.016 (5%).

Table A4. Test Conditions for SL 5149 Trials

Vat temperature = 30°C
Ambient temperature = 23.0°C
Relative humidity at 23.0°C = 45%
Laser power at vat = 16 mW
Exposure time = 10 ms
Number of exposures = 2
Delay time between the two exposures = 1s
Strand length = 8 mm

Table A5. Summary of SL 5149 Linear Shrinkage Measurements

	Trial 1	Trial 2	Trial 3	Average	Standard Deviation
Strand width (mm)	0.181	0.185	0.184	0.183	
Final cure depth (mm)	0.309	0.302	0.307	0.306	0.0036
Final shrinkage (%)	1.33	1.32	1.36	1.34	0.021

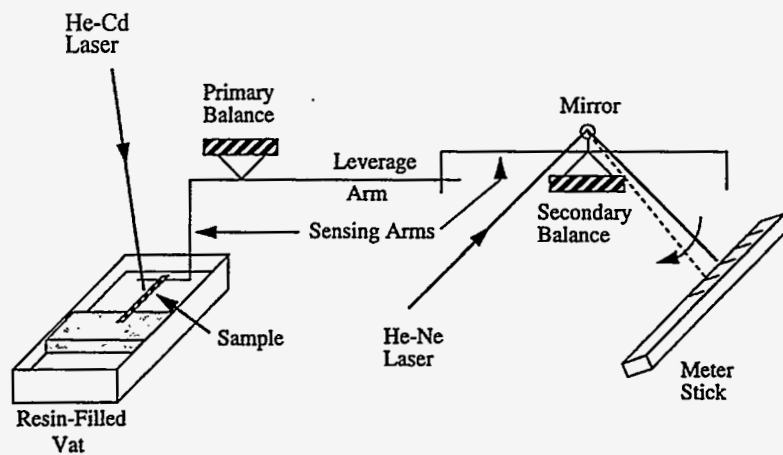


Figure A1. Schematic of the University of Dayton apparatus for measuring real time shrinkage during curing.

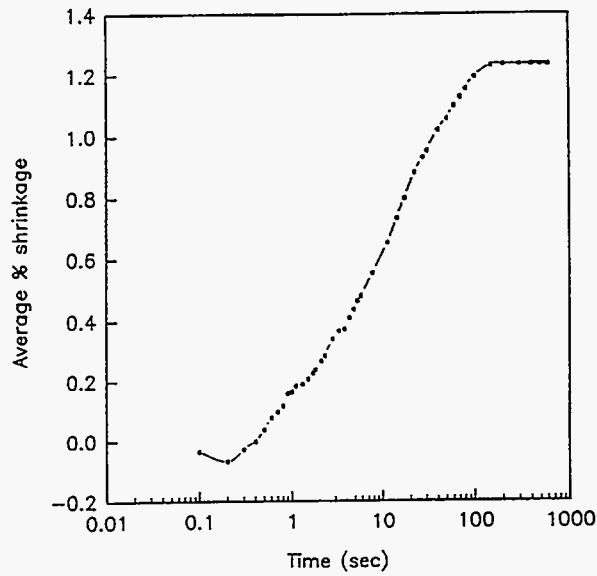


Figure A2. SL 5170 epoxy resin shrinkage vs log time; the data are averages of the four trials. The first 30 ms exposure occurs at time zero and the second 30 ms exposure occurs at 300 s.

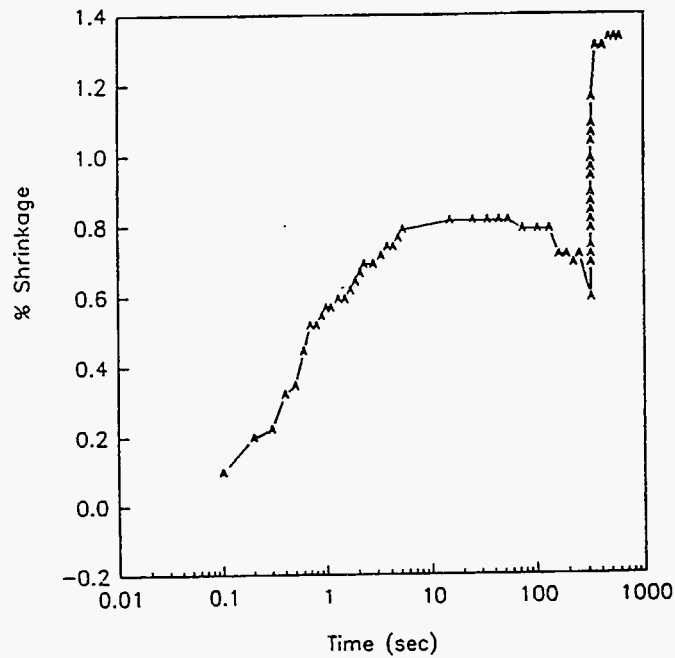


Figure A3. SL 5149 acrylate resin shrinkage vs log time for trial having a 5 minute wait between 10 ms exposures. (Vat temperature = 30°C, relative humidity = 40% measured at 23°C, and laser power at the vat = 16mW.)

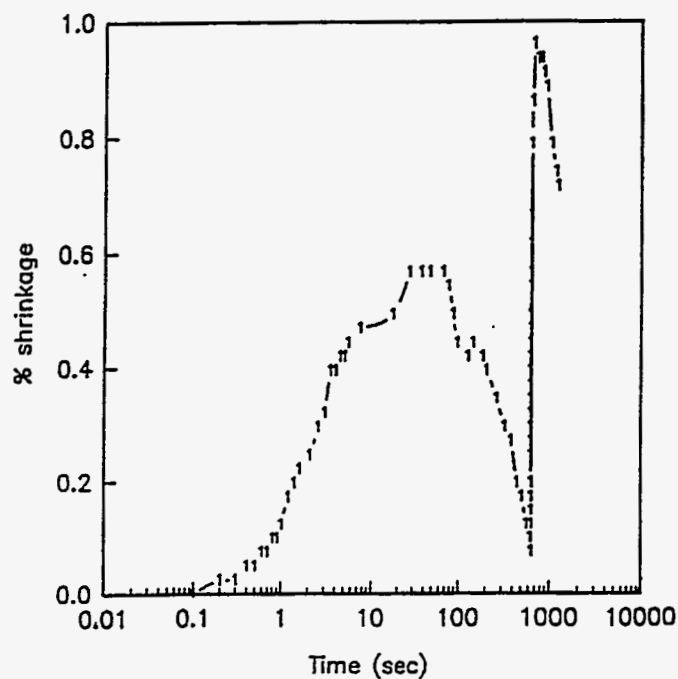


Figure A4. SL 5149 acrylate resin shrinkage vs log time for trial having a 10 minute wait between exposures. Data was collected for 10 minutes after second exposure. (Vat temperature = 30°C, relative humidity = 34% measured at 22°C, and laser power at the vat = 16mW.)

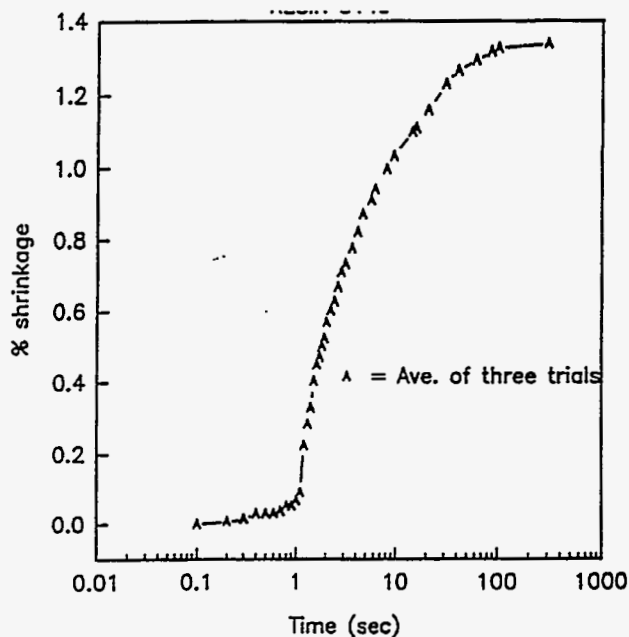


Figure A5. SL 5149 acrylate resin shrinkage vs log time for trial having a 1 second wait between the two 10 ms exposures.

APPENDIX B.

SL 5170 Epoxy: Stress-Strain Behavior of Single Strands and Bulk Material

In addition to in situ strand tests discussed in the body of this report, tests were performed on ultraviolet (UV) cured strands of SL 5149 acrylate and bulk specimens of SL 5170 epoxy. Results from these tests are reported in this appendix.

TENSILE TESTS:

SL 5149 acrylate strands

Four inch long epoxy strands were drawn in the SLA-250 apparatus, removed from the resin vat after 5 minutes, cured for 1 hour in a ultraviolet (UV) oven, then loaded in tension in an Instron test frame. When the strands were drawn: the resin temperature was 28C, the room relative humidity was 24% and the laser power 33 mW. In the tension tests, strand specimens with a 3.0 inch gage length were loaded to about 250 grams at three different strain rates. The specimens did not break at this maximum load. Stress-strain responses as a function of strain rate are plotted in Figure B1. Stresses are based on the average cross sectional area of a strand drawn with a single laser pass. Values of initial modulus for these strands are listed in Table B1.

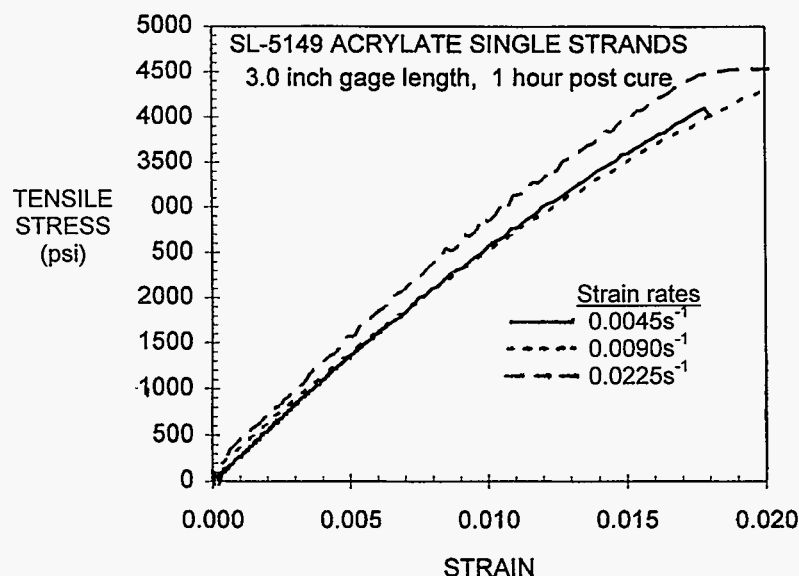


Figure B1. Tensile stress-strain responses of UV-cured SL 5149 acrylate single strands as a function of strain rates. (excel/ldrd2/fy95/ssacry2.xls)

Table B1. Initial Modulus of SL 5149 Acrylate Strands as a Function of Strain Rate and Post Cure Time.

STRAIN RATE (s ⁻¹)	POST CURE TIME (minutes)	INITIAL MODULUS (psi)
0.0090	0	1,300
0.0045	60	285,000
0.0090	60	280,000
0.0225	60	295,000

SL 5170 epoxy dogbone samples

Flat dogbone tension specimens were built in an SLA machine using the Accurate Clear Epoxy Solid (ACESTTM) build style [6], then cured for 1 hour in a UV oven. Specimens had final nominal dimensions of 6.0 inches length, 1.0 inches width, and 0.39 inch thickness. In the reduced-size gage section the width was 0.32 inch and length was 2.0 inches. Specimens were instrumented with a 1.0-inch extensometer in the gage section to measure strain. Testing procedures followed the guidelines in *ASTM D-638, the Standard Method of Test for Tensile Properties of Plastics*. Tensile loads were introduced into the specimens by means of wedge grips with serrated faces using a screw-driven Model 1125 Instron test machine. Typical stress-strain responses at three strain rates are shown in **Figure B2**; the response is nonlinear. Elastic moduli are taken as the initial tangent values of the stress-strain; these moduli are listed in **Table B2**.

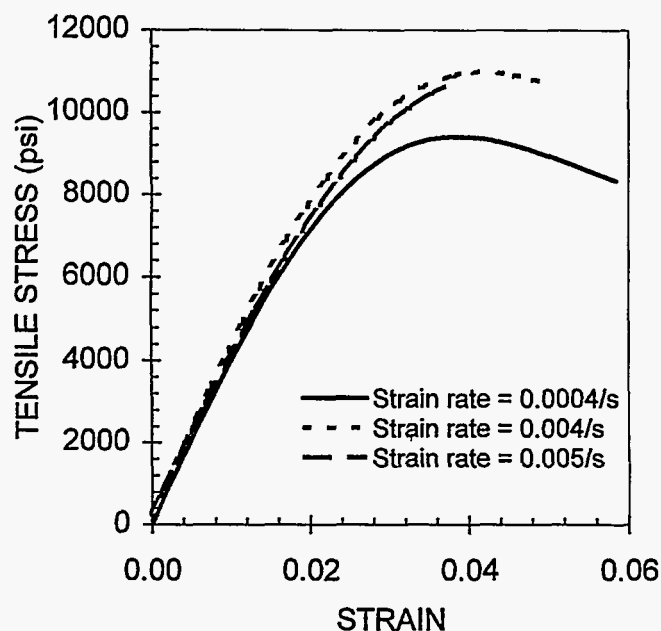


Figure B2. Typical tensile stress-strain responses of SL 5170 epoxy dogbone specimens as a function of strain rate. (excel\ldrd2\gregory.xls)

Table B2. Tensile Properties of SL 5170 Epoxy as a Function of Strain Rate

STRAIN RATE (s⁻¹)	MODULUS (psi)	STRESS at 0.2% YIELD (psi)	FAILURE STRESS (psi)
0.0004	424,000	6,360	8,360
0.004	445,000	7,235	11,060
0.005	445,000	7,430	11,150

ULTRASONIC TESTS:SL 5170 Epoxy

Ultrasonic wave speed measurements were made in the three principal orthogonal (X, Y, and Z) directions of cubic specimens built with the ACESTTM build pattern and cured for 1 hour in a UV oven. The edge dimensions of the cube was 0.75 inch. Longitudinal and shear wave velocities, along with specimen density of 1.18 g/cc, were used to calculate elastic constants in the three directions. The elastic properties based on ultrasonic wave speeds are listed in **Table B3**.

Table B3. Elastic Properties of SL 5170 Epoxy Calculated Using Ultrasonic Wave Speeds.

	X-DIRECTION	Y-DIRECTION	Z-DIRECTION
Young's Modulus (10⁶ psi)	0.558	0.559	0.560
Shear Modulus (10⁶ psi)	0.203	0.203	0.203
Bulk Modulus (10⁶ psi)	0.753	0.760	0.776
Poisson's Ratio	0.376	0.377	0.378

These ultrasonic elastic property measurements show that the stereolithography process for building SL 5170 epoxy parts produces a material that is isotropic. That is, the ultrasonic elastic moduli are identical in the three principal directions.

DISTRIBUTION

UNLIMITED RELEASE:

University of Dayton (3)
 Rapid Prototyping Development Lab
 Dayton, Ohio 45469-0130
 Attn.: Dr. Richard P. Chartoff
 Dr. Allan J. Lightman
 Dr. Jill S. Ullett

3D Systems (2)
 26081 Avenue Hall
 Valencia, CA 91355
 Attn.: Dr. Charles W. Hull
 Dr. Paul F. Jacobs

Dr. Manfred Hofmann
 Ciba-Geigy AG
 FZM-185.003, PO Box 64
 CH-1723 Marly-1
 Switzerland

MS 0320 4503 LDRD Office
 MS 0439 9234 D. R. Martinez
 MS 0439 9234 T. Hinnerichs
 MS 0439 9234 W. R. Witkowski
 MS 0841 9100 P. J. Hommert
 MS 0443 9117 H. Morgan
 MS 0443 9117 R. S. Chambers (10)
 MS 0960 1400 J. Q. Searcy
 MS 0961 1403 J. A. Sayre
 MS 0958 1471 G. D. McCarty
 MS 0958 1472 J. L. Ledman
 MS 0958 1472 J. A. Emerson
 MS 0958 1472 T. R. Guess (10)
 MS 0958 1472 M. E. Stavig

MS 0958 1484 C. L. Atwood (8)
 MS 0958 1484 M. L. Griffith
 MS 0958 1484 L. D. Harwell
 MS 0958 1484 P. G. Stromberg
 MS 0958 1484 B. T. Pardo
 MS 0958 1484 D. E. Reckaway
 MS 0615 2674 R. N. Shagam
 MS 0615 9752 J. H. Gieske
 MS 9402 8230 J. Spingarn
 MS 9018 8523-2 Central Technical
 Files
 MS 0899 4414 Technical Library (5)
 MS 0619 12615 Print Media
 MS 0100 7613-2 Document Processing
 For DOE/OSTI (2)

